Space-based near-infrared CO_2 measurements: Testing the Orbiting Carbon Observatory retrieval algorithm and validation concept using SCIAMACHY observations over Park Falls, Wisconsin

H. Bösch,[1] G. C. Toon,[1] B. Sen,[1] R. A. Washenfelder,[2] P. O. Wennberg,[2] M. Buchwitz,[3] R. de Beek,[3] J. P. Burrows,[3] D. Crisp,[1] M. Christi,[4] B. J. Connor,[5] V. Natraj,[2] and Y. L. Yung[2]

Received 17 January 2006; revised 20 June 2006; accepted 30 June 2006; published 6 December 2006.

[1] Space-based measurements of reflected sunlight in the near-infrared (NIR) region promise to yield accurate and precise observations of the global distribution of atmospheric CO_2. The Orbiting Carbon Observatory (OCO) is a future NASA mission, which will use this technique to measure the column-averaged dry air mole fraction of CO_2 (X_{CO_2}) with the precision and accuracy needed to quantify CO_2 sources and sinks on regional scales ($\sim$1000 $\times$ 1000 km^2) and to characterize their variability on seasonal timescales. Here, we have used the OCO retrieval algorithm to retrieve X_{CO_2} and surface pressure from space-based Scanning Imaging Absorption Spectrometer for Atmospheric Chartography (SCIAMACHY) measurements and from coincident ground-based Fourier transform spectrometer (FTS) measurements of the O_2 A band at 0.76 μm and the 1.58 μm CO_2 band for Park Falls, Wisconsin. Even after accounting for a systematic error in our representation of the O_2 absorption cross sections, we still obtained a positive bias between SCIAMACHY and FTS X_{CO_2} retrievals of $\sim$3.5%. Additionally, the retrieved surface pressures from SCIAMACHY systematically underestimate measurements of a calibrated pressure sensor at the FTS site. These findings lead us to speculate about inadequacies in the forward model of our retrieval algorithm. By assuming a 1% intensity offset in the O_2 A band region for the SCIAMACHY X_{CO_2} retrieval, we significantly improved the spectral fit and achieved better consistency between SCIAMACHY and FTS X_{CO_2} retrievals. We compared the seasonal cycle of X_{CO_2} at Park Falls from SCIAMACHY and FTS retrievals with calculations of the Model of Atmospheric Transport and Chemistry/Carnegie-Ames-Stanford Approach (MATCH/CASA) and found a good qualitative agreement but with MATCH/CASA underestimating the measured seasonal amplitude. Furthermore, since SCIAMACHY observations are similar in viewing geometry and spectral range to those of OCO, this study represents an important test of the OCO retrieval algorithm and validation concept using NIR spectra measured from space. Finally, we argue that significant improvements in precision and accuracy could be obtained from a dedicated CO_2 instrument such as OCO, which has much higher spectral and spatial resolutions than SCIAMACHY. These measurements would then provide critical data for improving our understanding of the carbon cycle and carbon sources and sinks.

Citation: Bösch, H., et al. (2006), Space-based near-infrared CO_2 measurements: Testing the Orbiting Carbon Observatory retrieval algorithm and validation concept using SCIAMACHY observations over Park Falls, Wisconsin, *J. Geophys. Res.*, *111*, D23302, doi:10.1029/2006JD007080.

[1]Jet Propulsion Laboratory, California Institute of Technology, Pasadena, California, USA.
[2]Division of Geological and Planetary Sciences, California Institute of Technology, Pasadena, California, USA.
[3]Institute of Environmental Physics, University of Bremen, Bremen, Germany.
[4]Department of Atmospheric Science, Colorado State University, Fort Collins, Colorado, USA.
[5]National Institute of Water and Atmospheric Research, Lauder, New Zealand.

0148-0227/06/2006JD007080

1. Introduction

[2] Carbon dioxide (CO_2) is the major anthropogenic greenhouse gas, contributing about 1.46 W m^{-2} to the global radiative forcing [*Intergovernmental Panel on Climate Change* (*IPCC*), 2001]. Atmospheric CO_2 has increased from a preindustrial value of about 280 parts per million (ppm) to more than 380 ppm mainly caused by fossil fuel combustion and land use change [*IPCC*, 2001]. Our current knowledge about the temporal and spatial variability of atmospheric CO_2 is mainly based on accurate in situ measurements from networks of surface stations such as the NOAA Global Monitoring Division (CMDL) Carbon Cycle-Greenhouse Gases (CCGG) Cooperative Air Sampling Network. Because of the sparseness of these stations, CO_2 sources and sinks can only be inferred with significant uncertainties [*Gurney et al.*, 2002; *Bousquet et al.*, 2000; *Fan et al.*, 1998]. Improved quantitative understanding of the distribution and variability of the sources and sinks, however, is essential for reliable predictions of future CO_2 levels.

[3] As shown by *Rayner and O'Brien* [2001] and others [*Houweling et al.*, 2004; *Olsen and Randerson*, 2004], space-based measurements of the column-averaged CO_2 dry-air mole fraction (X_{CO_2}), if acquired globally and bias free with a precision of 1% or better, will provide data that are beneficial in reducing the uncertainties of source/sink inversions. As pointed out by *Houweling et al.* [2004], on regional scales, e.g., for the tropics, the requirements on the measurement accuracy and precision can be significantly relaxed. The feasibility and characterization of space-based CO_2 measurements for existing and future missions has been extensively discussed in several publications [*Frankenberg et al.*, 2005; *Mao and Kawa*, 2004; *Chédin et al.*, 2003a; *Dufour et al.*, 2004; *Kuang et al.*, 2002; *O'Brien and Rayner*, 2002; *Buchwitz et al.*, 2000; *Park*, 1997]. Among the studied techniques, measurements of reflected sunlight in the near-infrared (NIR) wavelength range are most promising since they can provide accurate X_{CO_2} with a high sensitivity near the Earth's surface, i.e., where the carbon sources and sinks are located [e.g., *Kuang et al.*, 2002].

[4] The Orbiting Carbon Observatory (OCO) is a mission dedicated to the measurement of atmospheric CO_2 with the precision and accuracy needed to quantify CO_2 sources and sinks on regional scales ($\sim$1000 $\times$ 1000 km^2) and to characterize their variability on seasonal timescales [*Crisp et al.*, 2004]. OCO is scheduled to be launched in 2008 and fly in the EOS Afternoon Constellation (A-Train) with a 705 km Sun-synchronous orbit with a 16 day repeat cycle and 1320 LT equator crossing time. The OCO instrument consists of three bore-sighted grating spectrometers that measure sunlight reflected from the Earth's surface and scattered from the atmosphere. X_{CO_2} will be retrieved from the measured spectra of two NIR CO_2 bands at 1.61 μm and 2.06 μm and the O_2 A band at 0.76 μm with a resolving power between 17,000 and 20,000. The simultaneous retrieval of the O_2 A band and the two CO_2 bands constrains uncertainties in the atmospheric photon path and surface pressure, which is crucial for a retrieval of X_{CO_2} to the required high precision (better than 2.5 ppm) [*Kuang et al.*, 2002]. To detect and remove potential biases in X_{CO_2}, the space-based OCO retrievals will be validated against measurements from a network of ground-based solar-viewing NIR Fourier transform spectrometer (FTS) instruments. These FTS spectra allow X_{CO_2} retrievals using the same absorption bands as OCO, but with much higher spectral resolution, thus critically testing the spectroscopy of O_2 and CO_2 plus interfering H_2O. Furthermore, the FTS measurements are insensitive to aerosol or surface effects, e.g., surface bidirectional reflection distribution functions (BRDFs), so that potential biases in X_{CO_2} can be exposed.

[5] In recent years, midinfrared CO_2 measurements from space have become available from different instruments. *Chédin et al.* [2003b, and references therein] report mid-tropospheric CO_2 concentrations from measurements of the High Resolution Infrared Sounder 2 (HIRS-2) instrument aboard the NOAA 10 satellite. They have been able to reproduce the seasonal patterns of CO_2 measured by in situ aircraft instruments in the tropics [*Matsueda et al.*, 2002]. They estimate the precision of these measurements to be around 1% for monthly means and averaged over 15° $\times$ 15°. Similar results, but with an improved measurement precision of $\sim$0.8%, have been found by *Crevoisier et al.* [2004] using measurements of the Atmospheric Infrared Sounder (AIRS) instrument. *Engelen and McNally* [2005] have analyzed CO_2 from AIRS radiances with a data assimilation technique and they estimated a mean error on the order of 1% for a 5-day average on a 6° $\times$ 6° grid. Furthermore, *Chahine et al.* [2005] demonstrated that the 5 ppm seasonal variation inferred from the in situ aircraft instruments can be tracked from AIRS observations with an accuracy of 0.43 ± 1.20 ppm. A major limitation of these thermal emission measurements, however, is their lack of sensitivity to the lower troposphere.

[6] More recently, near-infrared CO_2 measurements have become available through the Scanning Imaging Absorption Spectrometer for Atmospheric Chartography (SCIAMACHY) instrument on Envisat [*Bovensmann et al.*, 1999; *Burrows et al.*, 1995]. SCIAMACHY was designed to provide global measurements of trace gases in the troposphere and in the stratosphere, including experimental measurements of CO_2 and CH_4. X_{CO_2} retrievals from SCIAMACHY measurements over land have been published by *Buchwitz et al.* [2005b, 2005a, 2004] for the year 2003 (SCIAMACHY/WFMD Version 0.4 X_{CO_2} data product). They found agreement with models within 15–30 ppm (standard deviation of the difference for individual measurements). The comparison focused on X_{CO_2} variability and not on absolute values because the CO_2 and O_2 columns had been scaled (by 1.27 and 0.85, respectively). Recent investigations have shown that the scaling of the CO_2 columns was necessary due to calibration problems of the Level 1 Version 4 spectra which have been used for SCIAMACHY/WFMD Version 0.4 X_{CO_2}. These problems have to a large extent been solved for Version 5 spectra [*Buchwitz et al.*, 2006] but the entire data set has not yet been reprocessed. *Dils et al.* [2006] compared (the scaled) Version 0.4 X_{CO_2} at three Fourier transform infrared (FTIR) stations and found a quite systematic low bias of about 7% and a scatter relative to FTIR of 3–4%. They estimate the accuracy of the FTIR CO_2 measurements to 3%. For different reasons, none of the three stations was ideal for such a comparison (Jungfraujoch is a high altitude station (complex terrain, boundary layer not observed), Ny Alesund is a high-latitude station (low

Sun, low snow/ice near-infrared albedo), and Egbert near Toronto is influenced by local sources). Using shipborne FTIR measurements, *Warneke et al.* [2005a] found agreement within about 5% by comparing a couple of days of nearby SCIAMACHY/WFMD Version 0.4 X_{CO_2} measurements over land (Africa) during end of January/beginning of February 2003.

[7] In this article, we compare X_{CO_2} and surface pressure retrieved from SCIAMACHY Version 5 spectra measured over Park Falls, Wisconsin, with those retrieved from colocated ground-based solar-viewing FTS spectra [*Washenfelder et al.*, 2006] analyzed with the OCO retrieval algorithm. We investigate potential biases in the SCIAMACHY X_{CO_2} retrievals and estimate the precision for Park Falls summer conditions. Since SCIAMACHY observations are similar in viewing geometry and spectral range to those of OCO, this study represents an important test of the OCO retrieval algorithm and validation concept. A limitation of this test, however, is that we had to modify the OCO retrieval approach (see sections 3 and 4.2) due to the lower spectral resolution of SCIAMACHY and the fact that we could not use the 2.0 μm CO_2 band. In particular, the treatment of aerosol scattering is significantly simplified compared to the approach that we plan to use for retrieving OCO spectra.

[8] This paper is organized as follows: In section 2, we describe the OCO retrieval algorithm followed by a description of the SCIAMACHY and FTS measurements in section 3. A discussion of our analysis procedure for the SCIAMACHY and FTS spectra can be found in section 4. In section 5 we show the results of the X_{CO_2} and surface pressure retrieval from SCIAMACHY and FTS spectra. We conclude with an assessment of the implications of these results for the OCO mission in section 6.

2. Retrieval Algorithm

[9] The OCO Level 2 retrieval algorithm is being developed to accurately retrieve the column-averaged dry air mole fraction of CO_2 (X_{CO_2}) from near-infrared radiance spectra. Although the retrieval algorithm will be primarily used for simultaneously fitting the O_2 A band at 0.76 μm and the CO_2 bands at 1.61 μm and 2.06 μm, it can be applied to many different retrieval problems. A flexible scheme allows the retrieved parameters to be selected from a large pool of atmospheric/surface/instrumental parameters and hence the retrieval strategy can be easily changed as required for other applications. The major components of the OCO retrieval algorithm, the forward model and the inverse method, are now described.

2.1. Forward Model

[10] The forward model **F** describes the physics of the measurement process and relates measured radiances **y** to the state vector **x**:

$$\mathbf{y} = \mathbf{F}(\mathbf{x}, \mathbf{b}) + \epsilon \tag{1}$$

where ϵ is the measurement error and **b** represents additional nonretrieved parameters. The state vector **x** contains all retrieved parameters. For retrieval from OCO spectra, **x** will include volume mixing ratios of CO_2 and H_2O, aerosol optical depth and temperature profiles, surface pressure, surface albedo and its first-order spectral dependence, spectral shift and spectral stretch/squeeze. Parameters that are not retrieved, but needed by the forward model, such as gaseous absorption cross sections or atmospheric parameters that are accurately known from other measurements, are described by the vector **b** (e.g., O_2 volume mixing ratio (vmr)). Errors in these parameters **b** will result in errors in the retrieved parameters and they have to be explicitly included in the error budget of the retrieval.

[11] The forward model consists of three major modules: a radiative transfer (RT) code, a solar model, and an instrument model. The current version of the retrieval algorithm uses the ''Radiant'' plane-parallel, multiple-scattering RT code [*Christi and Stephens*, 2004], which solves the radiative transfer equation with an adding eigenmatrix method. For a given atmospheric and surface state, we compute a monochromatic top-of-atmosphere transmission spectrum with a grid size of 0.01 cm^{-1}, which resolves the individual O_2 or CO_2 lines in the NIR with $\sim$2 points per minimum Doppler width. A unique feature of Radiant is the so-called layer-saving option that allows time efficient computation of the weighting functions $\mathbf{K} = \partial\mathbf{y}/\partial\mathbf{x}$, which are of central importance for the inverse method described in section 2.2. In layer-saving mode, Radiant stores the reflectance and transmission functions of each layer in memory. The calculation of a weighting function for a certain quantity, by a subsequent call to Radiant, then requires only recalculating the reflectance and transmission functions of the perturbed layer and not the whole atmosphere. Radiant does not take into account the polarization of the light caused by atmospheric scattering processes and reflection by the Earth's surface. A proper treatment of these effects requires computationally expensive polarized RT calculations. Neglecting polarization, in particular for polarization sensitive instruments such as OCO or SCIAMACHY, is known to cause errors [*Natraj et al.*, 2006], which are investigated in section 5.2.

[12] The solar model is based on an empirical list of solar line parameters which allows computation of a solar spectrum with arbitrary spectral resolution and point spacing. The use of a solar model avoids resampling a measured solar spectrum which would otherwise cause spectral artifacts due to the OCO and SCIAMACHY spectra being insufficiently oversampled [*Chance et al.*, 2005]. In the presence of significant calibration errors, which might be common to the solar irradiance and the radiance measurement, the use of a measured solar spectrum could be more favorable, since these calibration errors could partly cancel. The solar line list covers the range from 550 to 15,000 cm^{-1} and is derived from FTS solar spectra: Atmospheric Trace Molecule Spectroscopy (ATMOS) exoatmospheric and MkIV balloon spectra for the range 550–5650 cm^{-1} [*Geller*, 1995, 1992] and Kitt Peak ground-based spectra for 5000–15,000 cm^{-1} [*Wallace et al.*, 1993; *Livingston and Wallace*, 1991]. We have assembled two different line lists, representing the disk-integrated and the disk center solar spectrum. For the analysis of measurements of scattered or reflected sunlight, as carried out by OCO or SCIAMACHY, a disk-integrated solar spectrum is required. Direct solar-viewing instruments, on the other hand, typi-

cally point to the center of the solar disk with a field of view smaller than the diameter of the disk and a disk center solar model is required for their analysis. The disk center solar transmittance model has been used extensively for the analysis of ground-based FTS spectra in the IR [e.g., *Toon et al.*, 1999] and has more recently been applied to the NIR [*Yang et al.*, 2005; *Washenfelder et al.*, 2003; *Yang et al.*, 2002].

[13] The instrument model simulates the instrument's spectral resolution and spectral sampling by convolving the calculated, highly resolved, monochromatic radiance spectrum with the instrument line shape function (ILS) and subsequently with a boxcar function to take into account the spectral range covered by a detector pixel. The instrument model also enables one to account for potential intensity offsets or so-called channeling effects, a common artifact in FTS spectra that appears as a near-sinusoidal modulation in the spectral continuum.

[14] The retrieval algorithm has been designed to allow retrievals for different measurement geometries, e.g., nadir measurements from space or direct sunlight measurements from the ground. This feature allows us to use the same algorithm for the analysis of space-based and ground-based measurements for validation purposes, thus minimizing potential algorithmic biases. In the case of direct solar observations, the multiple-scattering calculation is replaced by a simple calculation of the transmission spectrum.

2.2. Inverse Method

[15] The inverse method is based on the optimal estimation technique [*Rodgers*, 2000] that constructs an optimal solution $\hat{\mathbf{x}}$ of the inverse problem (equation (1)) by minimizing the a posteriori cost function

$$\chi^2 = (\mathbf{y} - \mathbf{F}(\mathbf{x}))^T \mathbf{S}_\epsilon^{-1} (\mathbf{y} - \mathbf{F}(\mathbf{x})) + (\mathbf{x} - \mathbf{x}_a)^T \mathbf{S}_a^{-1} (\mathbf{x} - \mathbf{x}_a) \quad (2)$$

where $\mathbf{x}$ is the state vector, $\mathbf{y}$ is the measured spectrum, $\mathbf{S}_\epsilon$ is the measurement error covariance matrix, $\mathbf{x}_a$ is the a priori state vector, $\mathbf{S}_a$ is the a priori covariance matrix, and T is the transpose operator. We assume that $\mathbf{S}_\epsilon$ is diagonal and follows Gaussian statistics, both reasonable assumptions for OCO or SCIAMACHY measurements. Since the number of quantities that can be independently determined from the measurements is typically smaller than the number of state vector elements, the inverse problem does not have a unique solution and it is necessary to constrain the solution space. This is achieved by using the a priori state vector $\mathbf{x}_a$ and covariance matrix $\mathbf{S}_a$, which provide information about the climatological mean of $\mathbf{x}$ and its expected variability and correlations. The retrieved state $\hat{\mathbf{x}}$ will depend on the choice of $\mathbf{x}_a$ and $\mathbf{S}_a$, which has to be taken into account when interpreting the retrieval results.

[16] Because of the nonlinear nature of the retrieval problem, i.e., the weighting functions $\mathbf{K}$ depend on the state vector $\mathbf{x}$, we use an iterative Gauss-Newton scheme to obtain the optimal solution $\hat{\mathbf{x}}$. For each iteration step, the spectrum $\mathbf{y}$ and the weighting functions $\mathbf{K}$ are calculated with the forward model described earlier. After typically three to five steps, this iterative retrieval process has converged and the a posteriori error covariance $\mathbf{S}$ and the averaging kernel matrix $\mathbf{A}$ are calculated:

$$\mathbf{S} = \left(\mathbf{K}^T \mathbf{S}_\epsilon \mathbf{K} + \mathbf{S}_a^{-1}\right)^{-1} \quad (3)$$

$$\mathbf{A} = \mathbf{S}\mathbf{K}^T \mathbf{S}_\epsilon \mathbf{K} \quad (4)$$

The averaging kernel matrix gives the sensitivity of the retrieval to the true profile and is important for the interpretation and characterization of the retrieval results. Finally, we calculate X_{CO_2}:

$$X_{CO_2} = \mathbf{h}^T \hat{\mathbf{x}} \quad (5)$$

with the pressure weighting operator $\mathbf{h}$, whose elements are zero for all non-CO_2 elements. The error variance of X_{CO_2} and the column averaging kernel $\mathbf{a}$ are then given by

$$\sigma^2_{X_{CO_2}} = \mathbf{h}^T \mathbf{S} \mathbf{h} \quad (6)$$

$$\mathbf{a}^T = \mathbf{h}^T \mathbf{A} \quad (7)$$

3. Measurements

[17] We have retrieved X_{CO_2} from SCIAMACHY nadir spectra measured over Park Falls, Wisconsin (46°N, 90°W) and from correlative ground-based solar absorption FTS spectra, which are acquired at Park Falls next to the 450 meter tall television transmission tower (WLEF-TV). The WLEF-TV tower is also used for continuous in situ measurements of CO_2 concentrations at several altitudes and has been the subject of several intensive measurement and modeling studies [*Nicholls et al.*, 2004; *Denning et al.*, 2003; *Gerbig et al.*, 2003; *Berger et al.*, 2001]. The environment surrounding Park Falls is a heavily forested region dominated by boreal lowland and wetland forests. The relatively homogenous vegetation and the relatively low relief make this site well suited for intercomparison studies of space-based and ground-based measurements. Care has to be taken when using SCIAMACHY measurements over nearby Lake Superior (70 km to the north). The boundary layer CO_2 concentrations are typically higher over the Great Lakes during the daytime due to the absence of CO_2 sinks [*Nicholls et al.*, 2004]. In addition, the very low albedo of the water surface will degrade the precision of the measurement and will also give rise to a larger contribution of atmospheric aerosol scattering to the measured spectrum, which can potentially bias our X_{CO_2} retrieval if the true aerosol optical depth significantly differs from the assumed value of 0.1 (see discussion in section 5.2). It should be pointed out, that for bright surfaces, e.g., snow, aerosol scattering can enhance the photon path length due to the strongly forward peaked phase function, which can subsequently bias the retrieval of CO_2 [*Houweling et al.*, 2005].

3.1. SCIAMACHY Measurements

[18] SCIAMACHY is one of the instruments of the Envisat satellite launched in 2002. Envisat is in a Sun-synchronous orbit with an equator crossing time of 10 am local time. SCIAMACHY is a eight-channel grating spectrometer measuring sunlight scattered and reflected from the Earth in the spectral region from 0.24 to 2.4 μm [*Bovensmann et al.*, 1999]. Its viewing modes are nadir, limb, solar and lunar occultation. The integration time and thus the footprint size of nadir measurements varies from

channel to channel and is typically 30 × 60 km^2 for channels 4 and 6 and 30 × 120 km^2 for channels 7 and 8. SCIAMACHY also provides an extraterrestrial solar reference spectrum, which is obtained by measuring direct sunlight scattered into the instrument by a diffuser plate.

[19] For this study, we have selected SCIAMACHY Version 5 nadir spectra, which have been obtained between June and October 2004 and February and August 2005 for overpasses over Park Falls within a distance of 150 km. For each overpass, we have selected the observation whose ground pixel location is closest to Park Falls. Averaging a number of spectra would improve the precision of the retrieved X_{CO_2}, but would complicate the interpretation of systematic effects. SCIAMACHY measurements for the winter months with solar zenith angles (SZAs) larger than 60° are omitted to avoid errors due to the plane-parallel approximation in our current RT code. For our X_{CO_2} retrieval we have used SCIAMACHY spectra of the O_2 A band between 0.755 and 0.773 μm in channel 4 and of the CO_2 band between 1.562 and 1.595 μm in channel 6 with spectral resolutions of ~0.4 nm and 1.4 nm, respectively. In accordance with other groups [e.g., *Buchwitz et al.*, 2005a, 2005b] we do not use the 1.61 μm CO_2 band, that will be used by OCO. Both CO_2 bands are virtually identical in terms of their spectroscopy and this decision is based on the better performance of the SCIAMACHY detector around 1.58 μm, despite O_2 dayglow emissions potentially perturbing the measurements in this wavelength range [*Vallance Jones and Gattinger*, 1963]. The relatively low temperatures of the detectors in channels 7 and 8 resulted in significant ice formation, which has subsequently impacted important instrument calibration parameters such as ILS. To avoid errors in the X_{CO_2} retrieval due to these calibration uncertainties, we did not use the 2.0 μm CO_2 band in channel 7 (spectral resolution of ~0.2 nm).

[20] The SCIAMACHY Level 1 radiance spectra have been calibrated using a software developed at University Bremen and Netherlands Institute for Space Research (SRON), with the polarization correction turned off. A dead/bad pixel mask was inferred from spikes in the dark current measurements. From comparisons between SCIAMACHY and Medium-Resolution Imaging Spectrometer (MERIS) spectra, *Acarreta and Stammes* [2005] concluded that the reflectivity measured by SCIAMACHY in channel 4 has to be scaled by a factor of ~1.2. As described in section 4.1, we adjust our modeled solar spectrum to the solar spectrum measured by SCIAMACHY and thus we have accordingly scaled the radiances in channel 4. Unfortunately, no such intercomparison study is available for the spectral range of channel 6 and no scaling factor is applied.

3.2. FTS Measurements

[21] The ground-based FTS measurements were carried out with a Bruker 125 HR operated by the California Institute of Technology [*Washenfelder et al.*, 2006]. This instrument serves as the prototype for the demonstration of the OCO validation concept. The fully automated FTS system is housed in a mobile shipping container next to the WLEF-TV tower. A Sun tracker with an active pointing system, which is mounted on top of the container, directs sunlight from the center of the solar disk into the FTS instrument (field of view ~0.14°). The dual detector acquisition system of the FTS allows simultaneous measurements of direct sunlight covering the whole spectral range from 3900 to 15,625 cm^{-1} with a spectral resolution of 0.02 cm^{-1} (optical path difference of 45 cm). This system is also equipped with a weather station that measures pressure, humidity and temperature at the surface. The surface pressure is monitored using a Setra Systems, Inc. Model 270 pressure transducer (±0.3 hPa), which is periodically calibrated using a Princo Instruments, Inc. Model 453 mercury manometer. The FTS CO_2 measurements have been extensively compared to in situ profiles from the tower and aircraft by *Washenfelder et al.* [2006]. From these comparisons they estimate a measurement precision of the FTS CO_2 column of 0.1%.

4. Data Analysis

4.1. SCIAMACHY Solar Fit

[22] The first step in the analysis procedure is to fit the solar irradiance spectrum from SCIAMACHY, which allows verification of the solar model and the ILS. The shape and the parameters of the ILS have been derived from ground calibration. In particular, the determination of the shape of the ILS of SCIAMACHY is nontrivial since it is sampled with only ~2 pixels per full width at half maximum (FWHM) and recommendations made by different groups are not identical. We have decided to follow the recommendation of University of Bremen to use a Gaussian ILS for both channels [*Buchwitz and Burrows*, 2004], which depends on the FWHM only. The SCIAMACHY solar spectrum used for this retrieval has been compiled and made available by ESA/ESTEC for verification purposes. It has an improved calibration compared to the operational solar spectrum.

[23] There are six parameters that are retrieved from the solar fit: FWHM of the ILS; coefficients of a second-order polynomial for the scaling of the continuum; spectral shift and squeeze/stretch. The second-order polynomial is needed since we have assembled only a solar transmittance model so far, which does not appropriately describe the broadband shape of the solar spectrum. The inferred polynomial is then used together with the solar transmittance model for the analysis of the radiance spectra as described in section 4.2.

[24] The spectral fit given in Figure 1 shows that the calculated solar spectrum reproduces the SCIAMACHY measurement reasonably well. Some systematic features can be found in the residual of both spectral ranges, which most likely reflect uncertainties in the instrument calibration. The FWHMs provided by the SCIAMACHY Level 1 product are 0.43 nm and 1.32 nm for the O_2 A band and for the 1.58 μm CO_2 band, respectively. From our solar fit we obtained FWHMs of 0.40 nm and of 1.34 nm, which slightly differ from the official product. For all subsequent fits we have used these FWHMs for the convolution of the calculated spectrum with the ILS. Extending or reducing the spectral range of the fit does not significantly alter the results which shows the robustness of the obtained FWHMs.

4.2. SCIAMACHY Nadir Fit

[25] SCIAMACHY nadir spectra of the O_2 A band and the CO_2 band have been analyzed simultaneously with the

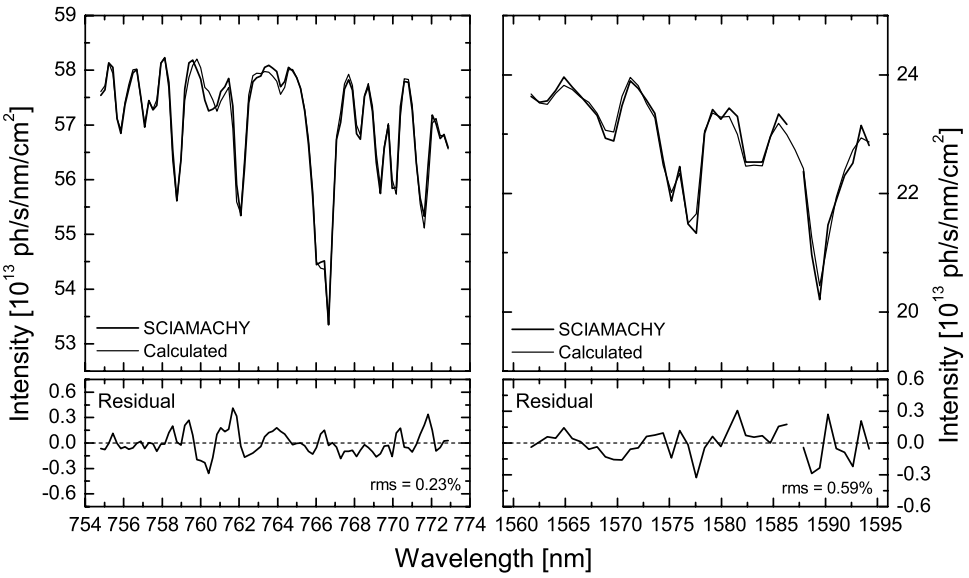

Figure 1. Spectral fit of the SCIAMACHY solar spectra in the spectral region of the O_2 A band and the 1.58 μm CO_2 band.

OCO retrieval algorithm. The parameters adjusted in the retrieval process are CO_2 vmr, water vapor vmr (absorbing in channel 6), surface pressure, surface albedo, first-order spectral dependence of the surface albedo, spectral shift and spectral squeeze/stretch. This is a subset of the parameters that will be retrieved from OCO spectra (section 2.1). The reason for reducing the number of state vector elements is the relatively low information content of the SCIAMACHY spectra due to its poorer spectral resolution and the unavailability of data from the 2.0 μm CO_2 band. Accordingly, instead of retrieving temperature and aerosol optical depth, we have used fixed values in our SCIAMACHY retrievals. We have used the temperature profile from National Centers for Environmental Prediction (NCEP) reanalysis for 1800 UT of each day. For the aerosol optical depth we used a constant value of 0.1 and 0.08 for the spectral region of the O_2 A band and the 1.58 μm CO_2 band, respectively. This agrees well with typical values of the aerosol optical depth at Park Falls measured by the Multiangle Imaging Spectroradiometer (MISR) and Moderate Resolution Imaging Spectroradiometer (MODIS) instruments, which rarely exceed 0.2. Optical properties of aerosol (spectral extinction and scattering coefficients and phase function moments) have been calculated with a Mie code based on work by *Wiscombe* [1980] for water-soluble aerosol [*Shettle and Fenn*, 1979] and a trimodal lognormal size distribution with mean radii of 0.004 μm, 0.13 μm and 0.26 μm. The vertical distribution has been assumed to be exponentially decreasing with a scale height of 1 km. Since X_{CO_2} is calculated from surface pressure retrieved from the O_2 A band and from the CO_2 profile retrieved from the 1.58 μm range, errors introduced by assumptions about the atmospheric aerosol loading will partly cancel out. A more detailed discussion about systematic errors can be found in section 5.2.

[26] The gaseous absorption cross sections have been precalculated on fixed pressure levels. A pressure interpolation to the retrieved surface pressure is carried out for the lowest level. For each pressure level, we have generated a set of nine cross sections by shifting the temperature by ±40 K in steps of 10 K from a typical midlatitude profile. Subsequently, the cross sections are interpolated to the NCEP atmospheric temperature. Errors introduced by this interpolation are insignificant since both absorption bands (O_2 and CO_2) are ground state transition that depend only weakly on temperature, especially the strongest lines. The spectroscopic line parameters for O_2 and H_2O have been taken from HITRAN 2004 [*Rothman et al.*, 2005]. Line parameters for CO_2 are from Toth et al. (personal communication, 2005), which have slightly improved positions and strengths relative to HITRAN 2004.

[27] The inversion as well as the forward model calculation uses 12 atmospheric pressure levels, with eight levels being in the troposphere. CO_2 vmrs are retrieved separately for each level, whereas for water vapor a single scaling factor is retrieved for the entire profile. The a priori CO_2 profile is taken from the MATCH/CASA model calculations [*Olsen and Randerson*, 2004] and the a priori humidity profile is from the European Centre for Medium-Range Weather Forecasts (ECMWF) ERA-40 data set both for Park Falls summer conditions. The a priori covariance used to constrain the CO_2 retrieval has been constructed from the MATCH/CASA model output for Park Falls summer conditions and has been scaled to produce a CO_2 column variability of ~35 ppm (~9%) (see the auxiliary material).[1] We have chosen a relatively loose constraint so that the dependence of the CO_2 retrieval for the lowest levels is small. The contribution of the constraint increases with altitude and above ~20 km (or ~50 hPa) the retrieval is dominated by the a priori profile (see also section 5.1). All other retrieved parameters have little sensitivity to the constraint and simple ad hoc constraints have been used.

[28] Clouds impose a major perturbation on our X_{CO_2} retrieval and we have avoided retrievals for cloudy scenes

[1] Auxiliary material is available at ftp://ftp.agu.org/apend/jd/2006jd007080.

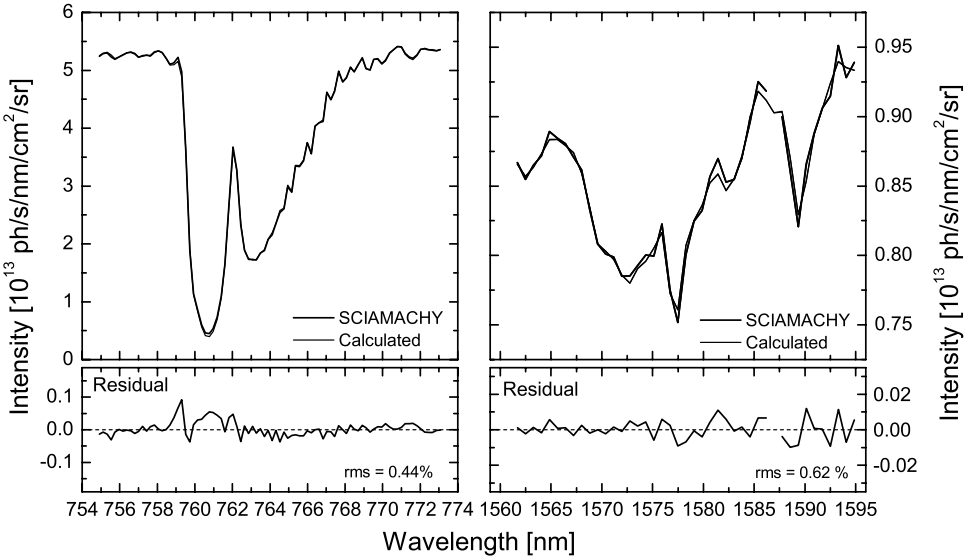

Figure 2. Spectral fit of the SCIAMACHY nadir spectra of the O_2 A band and the 1.58 μm CO_2 band over Park Falls, Wisconsin on 12 July 2004.

by carrying out a simple threshold test. All observations with a retrieved surface pressure of less than 900 hPa, which corresponds to a cloud top height of ~450 m above surface, have been assumed to be cloudy and have been discarded. Nevertheless, it is very likely that some of the observations that have passed this test still contain some minor cloud perturbations.

[29] A typical example of the spectral fit to a nadir spectrum is shown in Figure 2. The RMS of the fits is ~0.5%, which is a factor of ~3 larger than the theoretical noise level [*Buchwitz and Burrows*, 2004]. In the region of the O_2 A band, two distinct features can be identified: (1) Strong systematic structures are present at 0.759 μm and 0.762 μm, where large gradients in intensity occur and (2) calculated radiances are too large in the R branch around 0.761 μm and too small in the P branch around 0.765 μm. A likely cause for finding 1 is the uncertainty in the shape of the ILS. Line mixing, which is known to occur at the band head of the A band [*Yang et al.*, 2005] might also contribute to these structures. Finding 2 could be corrected to a large extent by adding a 1% intensity offset to the calculated spectra, which could arise from uncorrected instrument straylight. However, this seems to contradict *Lichtenberg et al.* [2005], who found a contribution of uniform straylight not larger than 0.1% from the on-ground calibration of SCIAMACHY. Also, neglecting polarization in the forward model will also cause spectral structures in the range of the A band, but with a magnitude much smaller that the observed residual structures. The same is true for atmospheric O_2 dayglow emissions and rotational Raman scattering, which contribute to the observed residual of the spectral fit (C. E. Sioris, Impact of the dayglow and the Ring effect on the retrieval of surface pressure from the A and B bands of O_2: Application to Orbiting Carbon Observatory, 2003, available at http://oco.jpl.nasa.gov/project-pubs.html). Another possible explanation for this residual structure is thin cirrus clouds or aerosol layers at high altitude, which can scatter sunlight into the field of view of the instrument in the saturated O_2 lines of the R branch. However, since the spectral residual shown in Figure 2 is similar for all our retrievals, it is unlikely that cirrus and high-altitude aerosol are the major reason for the observed artifacts. In summary, it is difficult to find a single reason for finding 2 and possibly a combination of several smaller effects is responsible for the observed discrepancies in the O_2 A band region.

[30] In the spectral range of the CO_2 band, there is no clear correlation between the residual structures of the fit and the atmospheric absorption of CO_2 or H_2O. The spectral residuals of the nadir fit are very similar to those of the solar fit. Ratioing the nadir spectra with the measured solar spectrum instead of using a solar model would certainly decrease the RMS of the fit for this case. At the same time, this approach would result in additional undersampling artifacts as discussed in section 2.1, and this option is not considered further.

4.3. FTS Fit

[31] We have retrieved X_{CO_2} from ground-based FTS spectra using the same algorithm and spectral bands as for the SCIAMACHY X_{CO_2} retrieval described above. The very high spectral resolution of FTS spectra exposes errors in the spectroscopy. To minimize our sensitivity to such errors, we decided to retrieve the FTS spectra by scaling the a priori CO_2 profile instead of retrieving the full profile. This scaling retrieval imposes a so-called hard constraint on the retrieval since it restricts the solution space of the inverse problem. By introducing a mapping matrix, which is given by the a priori CO_2 profile, the retrieved scaling factor can be related to the full vertical CO_2 profile and a column averaging kernel can be calculated in a straightforward way [e.g., *Bowman et al.*, 2002]. Other parameters retrieved from the FTS spectra are scaling factors for H_2O, surface pressure, spectral shift and a scaling factor for the intensities and its first-order spectral dependence. The latter two parameters are necessary since the FTS measurements are not radiometrically calibrated. Direct sunlight measurements are insensitive to aerosol optical depth or surface

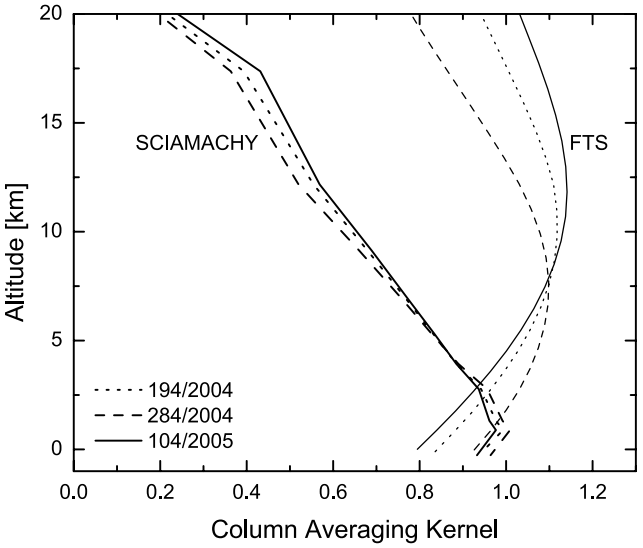

Figure 3. Column-averaging kernel for SCIAMACHY and FTS retrieval for three different observations (labeled with day of year and year).

albedo, hence these parameters are not retrieved. For more details about the FTS measurements we refer to *Washenfelder et al.* [2006] and *Yang et al.* [2005].

5. Results

5.1. SCIAMACHY-FTS Comparison

[32] In this section we discuss the retrieval results for X_{CO_2}, surface pressure and surface albedo obtained from SCIAMACHY and FTS measurements, analyzed with the same algorithm using the same spectral bands.

[33] A complication in comparing retrievals from spectra measured by different instruments is their different altitudinal sensitivities as expressed by their averaging kernels. Figure 3 shows the column averaging kernel for SCIAMACHY and FTS retrievals. For both instruments the averaging kernel is between 0.8 and 1 near the surface, where the largest variability of CO_2 is expected. The averaging kernel for SCIAMACHY strongly drops off with altitude, whereas the FTS kernel shows only a weak dependence on altitude for the lowest 20 km. These differences are mainly the result of the much higher spectral resolution of the FTS spectra and the differences between a full profile retrieval and a scaling fit. The effect of these kernel differences on the X_{CO_2} retrieval was assessed by a sensitivity analysis. If the true atmospheric CO_2 profile is $\mathbf{x}_{true}$ and the a priori CO_2 profile is $\mathbf{x}_a$, the retrieved X_{CO_2} can be estimated by

$$X_{CO_2} = X_{CO_2,a} + \mathbf{a}^T(\mathbf{x}_{true} - \mathbf{x}_a) \quad (8)$$

with the a priori dry air mole fraction $X_{CO_2,a}$ and the column averaging kernel **a**. We have constructed a 'true' CO_2 profile, by adding to the CO_2 a priori profile one standard deviation of the atmospheric CO_2 estimated from tower and aircraft in situ measurements at Park Falls [*Tans*, 1996]. Using the column averaging kernels for the FTS or SCIAMACHY retrievals as shown in Figure 3, we obtain a difference in retrieved X_{CO_2} from both instruments of up to 1–2 ppm. This intercomparison error does not dominate the overall error budget and so we did not attempt to reduce it by using the method developed by *Rodgers and Connor* [2003].

[34] The initial comparison of X_{CO_2} from SCIAMACHY and FTS is shown in Figure 4 (top, open symbols). FTS spectra were not available for all SCIAMACHY overpasses and, whenever possible, FTS spectra from other, nearby days were used to show the trend. Overall, we find a good qualitative agreement between SCIAMACHY and FTS, but with a positive bias of SCIAMACHY X_{CO_2} of up to 13 ppm. As expected, SCIAMACHY retrievals show a large scatter due to their relatively large retrieval errors. The 1-σ precision of the SCIAMACHY X_{CO_2} retrievals is only $\sim$10 ppm ($\sim$2.6%), which is roughly 30 times those of the FTS measurements. These retrieval errors have been calculated using the RMS of the fit residual and they are much larger than expected from theoretical signal-to-noise considerations [e.g., *Buchwitz and Burrows*, 2004]. Systematic structures, as seen in the SCIAMACHY fit residuals, will not necessarily translate completely into scatter in the retrieval, and hence our retrieval precision may overestimate the true precision. Some scatter in the space-based retrieval of X_{CO_2} is likely caused by deviations in atmospheric aerosol optical depth from the assumed constant value of 0.1, which will alter the atmospheric photon paths for the O_2 A band and the CO_2 band slightly differently (for a more detailed discussion see section 5.2).

[35] The surface albedo retrieved from SCIAMACHY spectra is given in Figure 4 (bottom). The surface albedo, which is mostly determined from spectral ranges without gas absorption, provides valuable information about the probed scenes. For a compilation of albedos for different surfaces and materials, see *Hook* [2000]. As expected for vegetated surface, we find a larger albedo for channel 4 than for channel 6 for most retrievals. Clear outliers such as day 245 in 2004 point to scenes with low clouds or fog, which have passed the applied cloud filter. Snow covered surfaces in February and March 2005 increase the albedo in channel 4, whereas soundings over Lake Superior can be identified by a very small albedo in both channels (e.g., days 111 and 124 in 2005).

[36] Figure 4 (middle) compares surface pressure retrieved from SCIAMACHY and FTS spectra with the measurements of the pressure sensor (Setra 270 pressure transducer) at the FTS site. The surface pressures retrieved from the SCIAMACHY O_2 A band spectra have been corrected for atmospheric water vapor contributions, which can contribute up to 0.35% for Park Fall summer conditions. Both instruments, SCIAMACHY and FTS, clearly overestimate the atmospheric values measured by the pressure sensor. This overestimation is in the range of 2–2.5% for FTS retrievals and is somewhat smaller for SCIAMACHY retrievals. The surface pressures retrieved from SCIAMACHY show a distinct scatter, which is mostly the result of uncertainties in topography and atmospheric aerosol loading. The SCIAMACHY observations do not exactly match the location of the FTS site and topographic variations in the vicinity of Park Falls of about 200 m will add an uncertainties to the retrieved surface pressure of

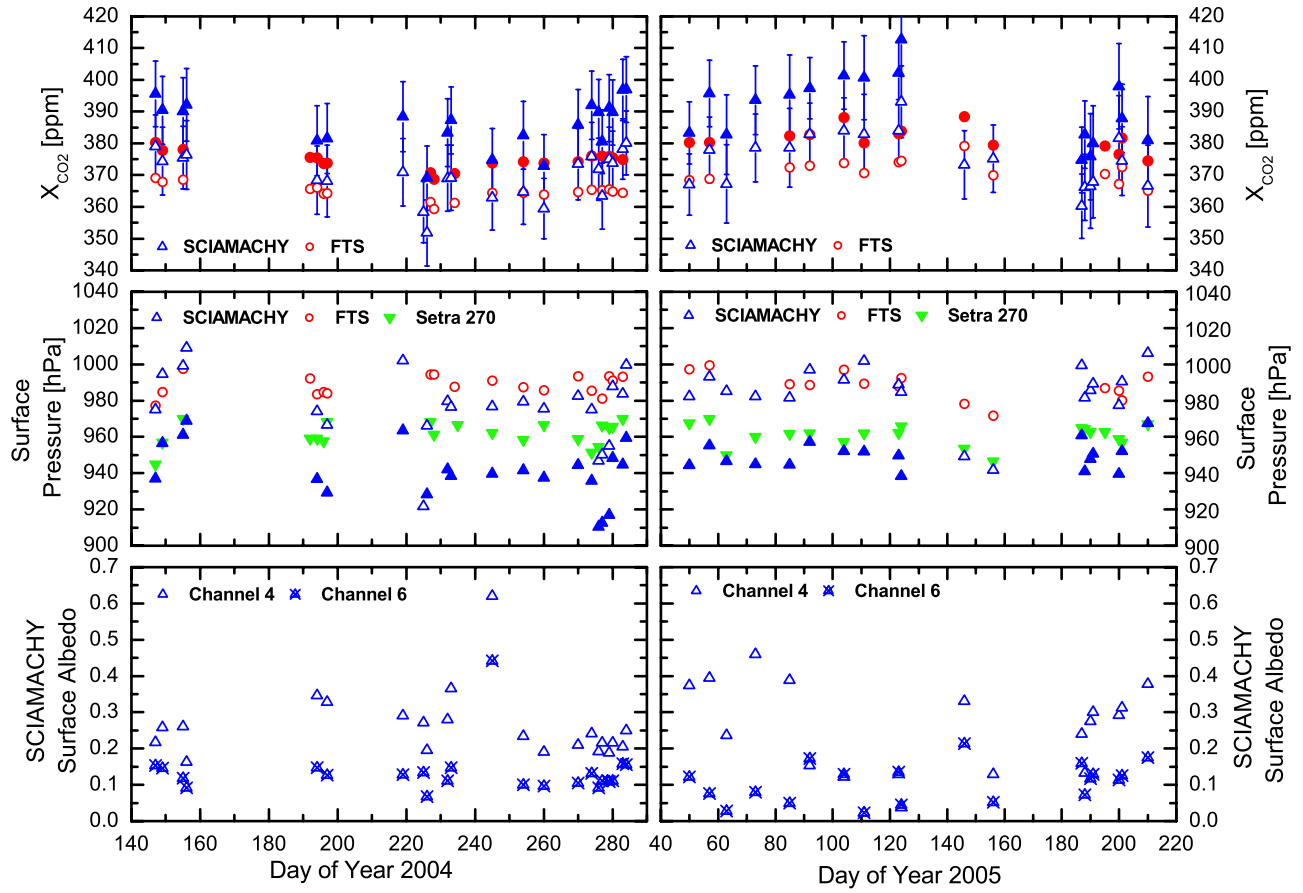

Figure 4. (top) Comparison of retrieved X_{CO_2} from SCIAMACHY and FTS spectra. Open symbols give the initial retrieval results, and solid symbols show X_{CO_2} retrieved from SCIAMACHY spectra using super-Lorentzian line shapes for O_2 and from FTS spectra using surface pressure measured by a calibrated pressure sensor at the FTS site (Setra 270 pressure transducer). (middle) Comparison of surface pressure from the initial SCIAMACHY and FTS retrievals to the surface pressure measured by the sensor. Also given is the surface pressure from SCIAMACHY retrievals using super-Lorentzian line shapes for O_2. The retrieved surface pressure has been corrected for water vapor contributions. (bottom) Retrieved surface albedo from SCIAMACHY for the initial retrieval. The errors (not shown) for X_{CO_2} from FTS are ~0.1%, for surface pressure ~0.02% and ~0.3% for FTS and SCIAMACHY, and for surface albedo ~0.1% and ~0.3% for channel 4 and channel 6.

about 25 hPa. Also variabilities in atmospheric aerosol loading and cloud perturbations directly affect the space-based retrieval of surface pressure.

[37] From an analysis of A band spectra measured by a ground-based FTS, *Yang et al.* [2005] found that using a Voigt line shape for the O_2 lines results in an overestimation of the O_2 column by a few percent. They subsequently invoked a super-Lorentzian far-wing line shape to bring the retrieved O_2 column into better agreement with reality. As suggested recently by *Tran et al.* [2006], collision-induced absorption and to a minor degree line mixing are most likely the major causes for the observed discrepancy. If not corrected, such inadequacies in the description of the O_2 A band spectroscopy will result in systematic errors in the surface pressure retrieval and will consequently bias the retrieval of X_{CO_2}.

[38] To study the impact of this spectroscopic effect on our SCIAMACHY surface pressure retrievals, we have degraded high-resolution O_2 A band spectra measured by the ground-based FTS at Park Falls to SCIAMACHY resolution. Since the light path for direct sunlight measurement is known, we can directly attribute any error in the retrieved surface pressure to inadequacies in the Voigt line shape. Figure 5 compares the measured surface pressure (pressure sensor) with the retrieved surface pressure from ground-based FTS spectra when the original FTS resolution is used and when the spectra are degraded to SCIAMACHY resolution. We find a SZA-dependent overestimation of the true surface pressure by ~2.8% for the FTS and by ~4% for the SCIAMACHY resolution. The small resolution dependence arises because the retrieval from low-resolution measurements are more dependent on the equivalent width of the integrated O_2 A band absorption, which depends mainly on the far-line wings of the strongest lines, whereas the least squares retrievals from the high-resolution FTS spectra are more dependent on the centers of the weaker lines. In a next step, we analyzed the same spectra using super-Lorentzian line shapes as suggested by *Yang et al.*

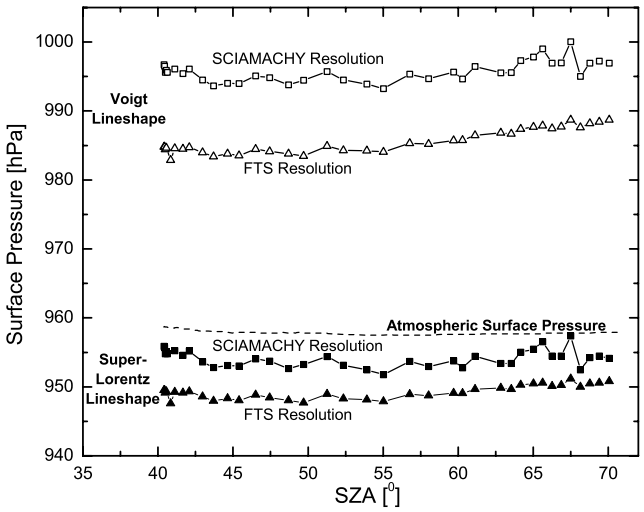

Figure 5. Surface pressure retrieved from ground-based FTS measurements on 6 October 2004 when the original FTS resolution is used and when the FTS spectra are degraded to SCIAMACHY resolution. We have used two different descriptions for the line shape of the O_2 lines. Results obtained for Voigt line shapes are given as open symbols and for super-Lorentzian line shapes as solid symbols. The atmospheric surface pressure given in the figure is measured at the FTS site with a Setra 270 pressure transducer.

[2005]. Now the retrieved surface pressure is much closer to truth (Figure 5) with an underestimation between 0.4% and 1% depending on spectral resolution.

[39] For ground-based FTS measurements, these spectroscopic uncertainties can be avoided by using surface pressure measured by the pressure sensor at the FTS site. However, for space-based measurements, surface pressure has to be retrieved to account for real changes in photon path length due to variations in topography and scattering. Consequently, we decided to adopt super-Lorentzian line shapes for O_2 lines for our SCIAMACHY retrievals, and similar to *Yang et al.* [2005], we have scaled the line strength by 0.99 (or the surface pressure with 0.995) to empirically compensate for the small underestimation of surface pressure as observed in Figure 5. Furthermore, we have convolved the super-Lorentzian line shape with a Gaussian line shape to take into account the Doppler effect. Super-Lorentzian line shapes have an effect which is very similar to those of collision-induced absorption, i.e., the far line-wing absorption is increased by an amount that scales with the square of the pressure, and it will appropriately correct ground-based and space-based observations, particularly since the shape of the collision-induced absorption is believed to be independent of pressure and temperature [*Pfeilsticker et al.*, 2001]. A temperature dependence in the integrated strength of the collision-induced absorption could introduce some small errors. This empirical approach clearly improves the O_2 retrieval, but some uncertainties remain, which we estimate to be in the range of 0.5% of the retrieved surface pressure. To achieve further improvements in the accuracy of surface pressure retrievals a more physics-based solution has to be developed, e.g., as proposed by *Tran et al.* [2006].

[40] The results of the FTS and SCIAMACHY retrievals when adopting super-Lorentzian line shape for O_2 lines for SCIAMACHY and using surface pressure from the in situ sensor for FTS, are shown as solid symbols in Figure 4. Now, the surface pressure retrievals from SCIAMACHY are mostly lower than the pressure sensor measurements. For X_{CO_2}, we find a comparison between SCIAMACHY and FTS X_{CO_2} which is similar to the previous one, but with values shifted upward by $\sim$10–15 ppm. We still observe a clear tendency for SCIAMACHY to overestimate X_{CO_2} by about 3.5% as compared to the FTS.

5.2. Error Analysis

[41] As shown in section 4.2, the spectra of O_2 and CO_2 measured by SCIAMACHY cannot be fitted to a level comparable to the measurement noise. Instead, we find significant spectral structures in the fit residuals that are common to all retrieved spectra. Furthermore, our SCIAMACHY retrievals show systematic biases as discussed above. Both observations clearly point to inadequacies in our representation of the transfer of radiation through the atmosphere and/or the SCIAMACHY instrument. For the retrieval of SCIAMACHY spectra we have made the following assumptions, which can potentially bias the result: (1) constant aerosol optical depth profile of known type; (2) known temperature profile from NCEP; (3) neglect of polarization; (4) instrument parameters are perfectly known; (5) no cloud of fog perturbations; and (6) neglect of O_2 dayglow and Raman scattering.

[42] Furthermore, errors in O_2 and CO_2 spectroscopy can bias the X_{CO_2} retrieval from FTS and SCIAMACHY spectra differently and thus can impede the intercomparison of both instruments. Currently, the major spectroscopic uncertainty is collision-induced absorption and line mixing in the O_2 A band. As discussed in section 5.1, this effect can be mostly corrected by adopting super-Lorentzian line shapes and we estimate that there is a remaining uncertainty in retrieved surface pressure of $\sim$0.5%. Uncertainties in the width and strength of O_2 A band lines have a similar effect on the FTS and SCIAMACHY retrievals. As a result of the strong O_2 absorption, a 1% error in width or strength will each yield a 0.5% error in retrieved surface pressure. For spectroscopic errors in CO_2 the situation is different. Because of the differences in the averaging kernels (see Figure 3) for the SCIAMACHY and the FTS retrieval, a line strength error will translate in somewhat different biases in retrieved X_{CO_2}. For the FTS spectra, this bias in X_{CO_2} will be similar to the error in line strength, whereas it will be significantly smaller for SCIAMACHY spectra due to the stronger effect of the a priori constraint. An error in the width of CO_2 lines typically results in a bias in X_{CO_2} which is much smaller than the error in width. In summary, from the discussed spectroscopic uncertainties, line strength of CO_2 has the biggest potential to bias the presented SCIAMACHY-FTS comparison, which can be up to 2–3 ppm for an assumed uncertainty of 1%.

[43] We have assessed potential biases in X_{CO_2} and surface pressure introduced by assumptions 1–4 in more detail with an linear error analysis, but first we discuss briefly the potential impact of assumptions 5 and 6. A low-

Table 1. Summary of the Linear Error Analysis of the SCIAMACHY Retrieval[a]

	Day	ILS		Abs	Rel Gain		Offset			Aerosol			
	and Year	Ch4	Ch6	Gain	Ch4	Ch6	Ch4	Ch6	T	τ	Type	h_{scale}	Pol
Δb		5%	5%	5%	1%	1%	1%	1%	2K	100%	-	+1km (+3km)	-
X_{CO_2},	194/04	0.4	0.4	0.3	0.07	0.01	4.3	2.4	0.08	0.1	0.35 (0.2)	0.2 (0.3)	0.08
ppm	284/04	1.0	0.6	0.8	0.2	0.03	6.2	3.3	0.09	0.06	0.08 (0.2)	0.4 (1.7)	1.1
	104/05	1.1	0.4	1.0	0.2	0.02	6.4	3.3	0.07	0.5	0.7 (0.03)	1.8 (5.8)	1.8
p_{surf},	194/04	1.4	0.	1.4	0.3	0.	16.5	0.	0.9	0.9	1.5 (0.4)	1.1 (0.6)	0.1
hPa	284/04	3.0	0.	3.0	0.6	0.	19.1	0.	0.8	0.8	0.2 (0.1)	4.2 (14.6)	4.0
	104/05	3.2	0.	3.2	0.6	0.	18.9	0.	0.9	1.8	2.0 (0.5)	7.3 (23.6)	6.3

[a]Errors in X_{CO_2} and surface pressure due to uncertainties in instrument calibration (ILS, absolute and relative radiometric gain and intensity offset), assumed atmospheric temperature, assumed aerosol characteristics, and due to neglecting polarization (Pol) are given. Also given are the assumed uncertainties Δb of the studied parameters. For ILS, relative gain and intensity offset, errors are given independently for channel 4 (Ch4) and channel 6 (Ch6). To investigate errors due to uncertainties in the atmospheric aerosol characteristics, we have changed the aerosol optical depth (τ), the aerosol type and the scale height (h_{scale}) of the vertical optical depth profile. The error due to aerosol type has been obtained by replacing the aerosol optical properties of the aerosol type used in the retrieval (see section 4.2) with those of water soluble aerosols with a monomodal distribution with a mean radius of 0.004 μm or dust-like aerosols with a bimodal distribution with mean radii of 0.13 and 0.3 μm (numbers in parentheses) [*Shettle and Fenn*, 1979].

altitude fog layer will impact the photon path length and can subsequently bias the space-based retrieval. Depending on particle type, vertical distribution and surface albedo, such a fog layer can either reduce the path length and partly shield the boundary layer or enhance the path length due to their forward peaked phase function. However, conditions in Park Falls in summer at 1030 LT are not dominated by fog or optical thick low-altitude aerosol layers and only a small number of the shown retrieval results should be affected. A similar effect will be caused by minor cloud perturbations such as thin cirrus clouds, which can pass the applied cloud filter. Raman scattering and O_2 dayglow both fill in strong O_2 absorption lines and contribute to the fitting residual, if not taken into account. As shown by C. E. Sioris (Impact of the dayglow and the Ring effect on the retrieval of surface pressure from the A and B bands of O_2: Application to Orbiting Carbon Observatory, 2003, available at http://oco.jpl.nasa.gov/projectpubs.html) the retrieval of surface pressure is essentially insensitive (within 0.4 hPa) to both of these effects, so we won't consider them further in this work.

[44] The linear error analysis technique [*Rodgers*, 2000] has been used to quantify biases caused by uncertainties in forward model parameters, i.e., parameters that are not retrieved, or by inadequacies in the forward model itself. The error covariance $\mathbf{S}_f$ of the retrieved parameters due to an error in nonretrieved parameters $\mathbf{b}$ can be obtained from

$$\mathbf{S}_f = \mathbf{G}\mathbf{K}_b\mathbf{S}_b\mathbf{K}_b^T\mathbf{G}^T \tag{9}$$

with the gain matrix $\mathbf{G}$, the weighting function $\mathbf{K}_b$ for the nonretrieved parameters and the error covariance $\mathbf{S}_b$, which has the assumed variances as diagonal elements. The gain matrix represents the mapping of the measurement variations into the state vector variations. $\mathbf{K}_b$ can be inferred in a straightforward manner by finite differences. All instrument parameters as well as temperature and aerosol optical depth and type are treated as nonretrieved parameters.

[45] The retrieval error due to the neglect of polarization is considered a forward model error $\Delta\mathbf{x}_f$, which can be expressed as:

$$\Delta\mathbf{x}_f = \mathbf{G}\Delta\mathbf{F} \tag{10}$$

where $\Delta\mathbf{F}$ is the error in the measured spectrum made by neglecting polarization. The error $\Delta\mathbf{F}$ is directly given by the difference of the intensities obtained with the nonpolarized RT code Radiant and a polarized RT code taking into account the polarization sensitivity of SCIAMACHY. This polarization sensitivity can be described by

$$I_{meas}(\lambda) = I(\lambda) + m_{12}Q(\lambda) + m_{13}U(\lambda) \tag{11}$$

where I_{meas} is the intensity measured by SCIAMACHY, I, Q and U are elements of the Stokes vector and m_{12} and m_{13} are elements of the instruments Müller matrix normalized to element (1,1) [*van Diedenhoven et al.*, 2005]. The polarization RT calculation has been carried out with the adding code for polarized light by *de Haan et al.* [1987] using the same atmosphere as for the nonpolarized RT calculation and a nonpolarizing Lambertian surface.

[46] Table 1 gives the result of the linear error analysis for three different SCIAMACHY observations at Park Falls that represent different measurement conditions. Also given are the assumed uncertainties (square root of the variance) of the studied nonretrieved parameters. We have included the following instrument parameters: FWHM of the ILS; overall radiometric gain (of both channels); relative radiometric gain of each channel; intensity offset. Not surprisingly, the intensity offset is by far the most critical instrument parameter. In particular, channel 4 shows a very large sensitivity due to the presence of strong O_2 lines in this spectral range. Assuming an offset error in channel 4 of 1% of the continuum intensity yields biases of 4.3–6.4 ppm in X_{CO_2} and of 16.5–18.9 hPa in surface pressure, depending on the scene. For the assumed uncertainties, other instrument parameters lead to much smaller errors in X_{CO_2} of around 1–2 ppm and in surface pressure of up to 6.5 hPa. Furthermore, Table 1 shows that the errors introduced by using NCEP temperatures are negligible assuming an accuracy of better than 2 K. To quantify potential errors due to assumption 1, we have included aerosol optical depth, aerosol scale height and aerosol type in the error analysis. As shown by Table 1, the assumption of a constant aerosol optical depth of 0.1 introduces only a small error in X_{CO_2} of less than 1 ppm for atmospheric aerosol loadings typically found at Park Falls of 0.1–0.2. As shown by *Houweling et al.* [2005] for regimes with very large aerosol optical depth such as the Sahara desert, the error caused by nonproper

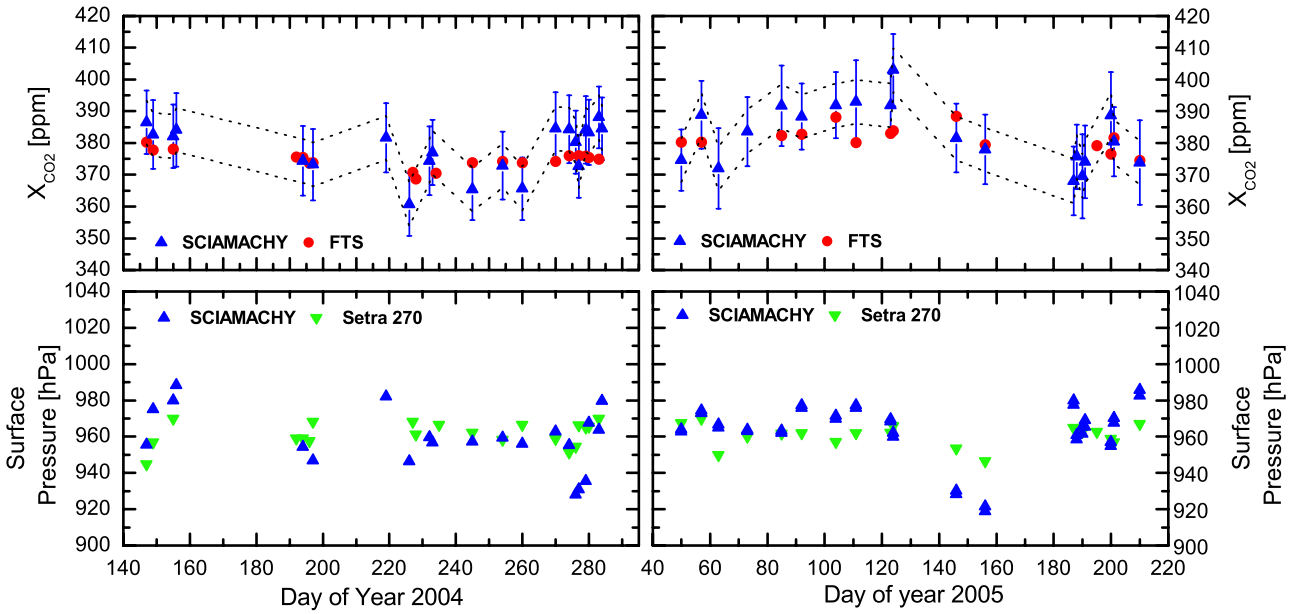

Figure 6. (top) Comparison of retrieved X_{CO_2} from SCIAMACHY and FTS spectra when a 1% intensity offset is added to the calculated SCIAMACHY O_2 A band spectra. The FTS results are identical to those shown as solid symbols in Figure 4. The dotted lines reflect the precision of the SCIAMACHY X_{CO_2} retrieval estimated from the correlation with the FTS retrievals (6.9 ppm or 1.8%). (bottom) Comparison of surface pressure retrieved from SCIAMACHY spectra (corrected for water vapor) with the pressure sensor (Setra 270 pressure transducer) measurements.

treatment of aerosol can be up to 10%. For the investigated aerosol types, errors due to assuming a certain aerosol type tend to be small (<0.7 ppm). Larger potential errors are found for uncertainties in the vertical distribution of aerosol. If the scale height is increased by 3 km, the errors in X_{CO_2} and surface pressure can be up to 5.8 ppm and 23.6 hPa, respectively, but they also show a very large variability for the different scenes. Neglecting polarization leads to an error in X_{CO_2} as large as 1.8 ppm. Since polarization depends on measurement geometry and surface albedo, neglecting polarization potentially introduces a geographically coherent bias in X_{CO_2} and surface pressure. More general studies of errors in CO_2 retrievals from SCIAMACHY due to aerosol scattering and temperature effects are given by *Frankenberg et al.* [2005], *Houweling et al.* [2005], and *Buchwitz and Burrows* [2004].

5.3. Modified SCIAMACHY Analysis

[47] As discussed in section 4.2, adding an intensity offset to the calculated O_2 A band spectra could be used to correct for spectral artifacts observed in the fit residual. The error analysis, however, has shown that the retrieval of X_{CO_2} is very sensitive to such an intensity offset. To demonstrate the effect on the retrieval, we have invoked a speculative intensity offset of 1% of the continuum intensity. In addition to the improved spectral fit of the O_2 A band with a RMS of the residual that is smaller by ~10%, we observe a much better agreement of X_{CO_2} and surface pressure from SCIAMACHY retrievals with the FTS retrievals and the pressure sensor measurements, respectively (Figure 6). From the correlation of X_{CO_2} from SCIAMACHY with FTS we infer a precision of ~6.9 ppm or 1.8% for the SCIAMACHY retrievals and a small remaining bias of ~1%. Taking into account the variability of the atmospheric aerosol loading and the effects of polarization would likely further shrink the observed scatter in SCIAMACHY X_{CO_2} and improve the inferred precision. The surface pressure retrieved from SCIAMACHY is now in reasonable agreement with the sensor measurement taking into account the expected variability due to topographic and scattering effects.

[48] The impact of intensity offset on the retrieval of SCIAMACHY O_2 A band spectra is also discussed by *van Diedenhoven et al.* [2005]. They have to add a ~1% intensity offset to bring the retrieval of apparent surface pressure from SCIAMACHY into agreement with Global Ozone Monitoring Experiment (GOME) and with simulation based on UK Met Office (UKMO) surface pressure. However, this has the opposite sign to the intensity offset that we use to improve our spectral fit of O_2. The reason for this discrepancy is not clear; however, both studies invoke an intensity offset based on very different analyses. When using Voigt lines and omitting an intensity correction for the SCIAMACHY retrieval, the comparison of surface pressure between the in situ sensor measurements and the SCIAMACHY as shown in Figure 4 is in qualitative agreement with the results of the study of *van Diedenhoven et al.* [2005] without intensity offset. However, *van Diedenhoven et al.* [2005] did not take into account the effects of non-Voigt line shapes of O_2 lines and so their retrieval of apparent surface pressure from GOME and SCIAMACHY might be somewhat biased toward larger values. Consequently, taking this effect into account would bring the SCIAMACHY retrieval into better agreement with their simulation and vice versa for GOME.

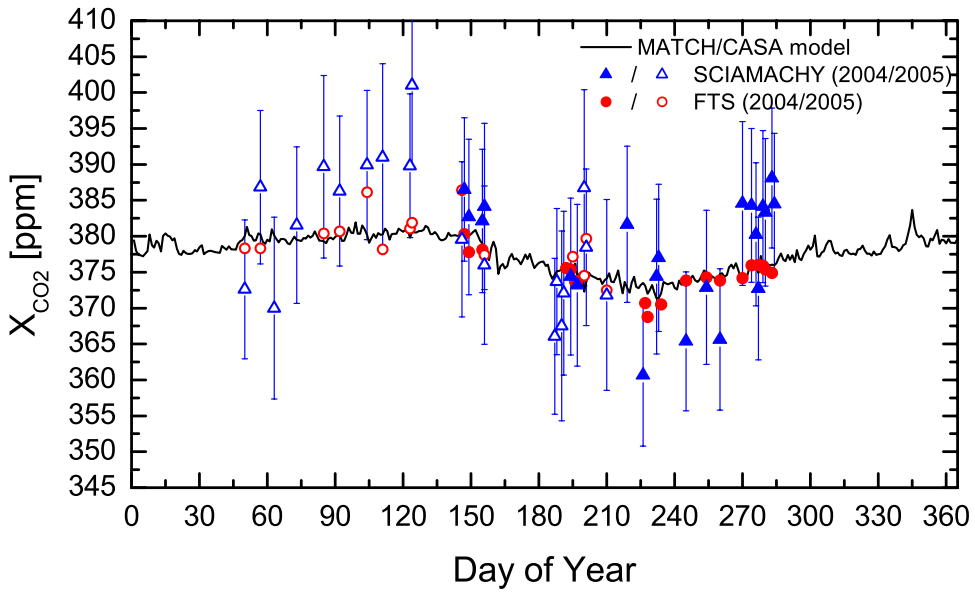

Figure 7. Comparison of X_{CO_2} for Park Falls retrieved from SCIAMACHY spectra and modeled with the MATCH/CASA model. The averaging kernels of the SCIAMACHY retrievals have been applied to the modeled CO_2 profiles. For comparison, the figure also gives X_{CO_2} retrieved from FTS spectra. The SCIAMACHY and FTS data are the same as in Figure 6; however, we have subtracted 2 ppm for 2005 to compensate the annual increase in atmospheric CO_2.

5.4. Comparison With Model Calculations

[49] We have compared the results of our modified SCIAMACHY X_{CO_2} retrieval (section 5.3) with the predictions of the MATCH/CASA model [*Olsen and Randerson*, 2004], that has been run for meteorological fields that represent a climatologically average year. The model includes CO_2 fluxes from fossil fuel emissions, gas exchange with the ocean and terrestrial net ecosystem production. No 'missing' carbon sink has been included. The model output has been spatially and temporally interpolated to the Park Falls location and 1030 LT, respectively. To obtain modeled X_{CO_2}, we have applied the SCIAMACHY column averaging kernels to these modeled CO_2 profiles, i.e., $\mathbf{x}_{true}$ in equation (8) is replaced with a modeled profile.

[50] Figure 7 shows modeled X_{CO_2} for Park Falls as a function of day of the year. The model nicely reproduces the typical shape of the seasonal cycle for the north hemispheric conditions with a maximum in May and a minimum in August. The modeled peak-to-peak amplitude is around 9 ppm. To illustrate the seasonal cycle from SCIAMACHY retrievals we show X_{CO_2} for the years 2004 and 2005 as a function of day of year only. The annual increase in atmospheric CO_2 has been compensated by subtracting 2 ppm from the 2005 columns [*Tans and Conway*, 2005]. For comparison, Figure 7 also shows the FTS X_{CO_2} retrievals displayed in the same way as the SCIAMACHY data. The different averaging kernel of the FTS retrieval is not taken into account here, but as noted earlier, this is expected to yield an error no more than 1–2 ppm. The seasonal cycle inferred from SCIAMACHY and FTS retrievals qualitatively agrees with the model calculation. Both measurements indicate a seasonal amplitude larger than predicted by the model. The large scatter in retrieved X_{CO_2} shown in Figure 7, in particular in the SCIAMACHY data, makes a proper derivation of the seasonal amplitude difficult. Significant improvements could be achieved by averaging a large number of measurements instead of using individual soundings. Nevertheless, we estimate that the model calculations of MATCH/CASA underestimate the amplitude found from measurements at Park Falls by 30–50%. Similar observations have been previously reported by other studies. *Buchwitz et al.* [2005a, 2005b] infer from SCIAMACHY measurements an amplitude of the seasonal cycle in the northern hemisphere which is up to a factor of 4 larger than obtained from the TM3 model. A smaller underestimation of the amplitude of 20–40% is found from comparisons of ground-based FTS measurements at Ny Alesund and Kitt Peak with the MATCH model [*Warneke et al.*, 2005b; *Olsen and Randerson*, 2004].

6. Implications for the OCO Mission

[51] Considering that the SCIAMACHY instrument was designed to address a broad range of scientific objectives, including experimental measurements of CO_2 and CH_4, the X_{CO_2} retrievals shown in Figures 4 and 6 look promising and clearly demonstrate that space-based near-infrared measurement are well suited to infer atmospheric CO_2 columns. Furthermore, after optimizing the decontamination procedure, the icing on the detectors has been very significantly reduced. We expect that future use of additional data from the 2 μm CO_2 band in channel 7 will improve the SCIAMACHY X_{CO_2} retrievals.

[52] As shown in section 5.2, instrument calibration is of major importance and small uncertainties in the calibration parameters can introduce errors in X_{CO_2} of several ppm. Calibration parameters may potentially change after launch of the instrument. Thus a thorough prelaunch calibration can be insufficient. It is necessary to develop tools that

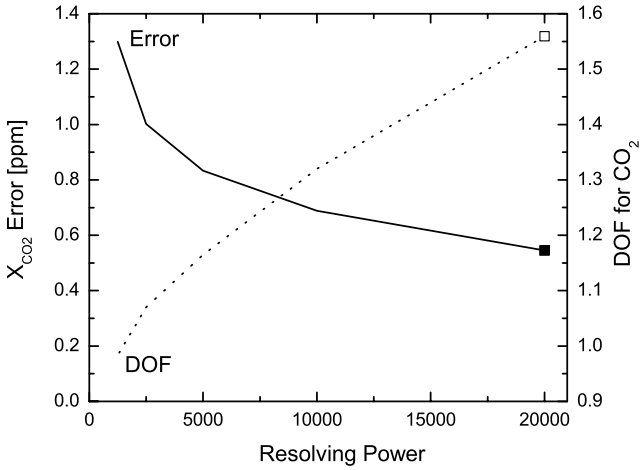

Figure 8. X_{CO_2} error and degrees of freedom (DOF) for CO_2 as a function of resolving power for an OCO-like instrument for Park Falls summer conditions. The resolving power is for the CO_2 bands only, the resolving power of the O_2 A band is 17.5% smaller. The square symbols represent the OCO instrument described in section 1.

allow verification and optimization of the calibration parameters in space. In particular, accurate knowledge of any potential intensity offset is crucial due to the strong atmospheric absorption of O_2 and CO_2.

[53] The OCO instrument will provide information about intensity offset from back-of-slit detector pixels, i.e., unmasked pixels that are not illuminated by the scene. These measurements will then be used to correct potential intensity offsets in the measured spectrum. For the ILS, we will rely mostly on the preflight calibration which will be performed with the technique developed by *Strow et al.* [2003]. As shown in section 4.1, a solar fit can be used to optimize the parameters (e.g., the FWHM) of the ILS of known shape. Since the sampling of the OCO ILS is only 2–2.5 pixels per FWHM, the solar fit will not allow a unique in-flight redetermination of the shape of the ILS. Finally, the in-orbit radiometric calibration of OCO will be based on measurements of the solar spectrum through an on-board diffuser and on vicarious calibration [e.g., *Abdou et al.*, 2002].

[54] As discussed in section 5.1, there are serious deficiencies in the spectroscopy of the O_2 A band due to the current lack of a proper description of collision-induced absorption and line mixing [*Tran et al.*, 2006]. Super-Lorentzian line shapes can be used to correct most of these deficiencies, but errors of the order of 0.5% of the retrieved surface pressure remain. Clearly, a more physics-based solution is preferable, e.g., as proposed by *Tran et al.* [2006]. As soon as such as solution becomes available we will implement it in the OCO retrieval algorithm. We also want to point out, that the high-resolution spectra of the ground-based FTS provide an excellent tool to test these changes in spectroscopy of O_2 since the O_2 air mass is precisely known.

[55] Achieving a precision and accuracy of better than 1% as needed for the retrieval of X_{CO_2} is difficult for instruments with relatively low spectral resolution and large footprints. We have calculated X_{CO_2} retrieval errors and the degrees of freedom (DOF) for CO_2 retrievals for an OCO-like instrument for Park Falls summer conditions as a function of spectral resolving power. The state vector now includes 61 elements, which are profiles with 12 levels for CO_2 vmr, H_2O vmr, aerosol optical depth and temperature, surface pressure and for each of the three OCO channels mean surface albedo, its first-order spectral dependence, spectral shift and spectral stretch/squeeze. The DOF are obtained from the trace of the averaging kernel matrix and gives the number of independent quantities that can be measured. For a resolving power of 20,000, the calculation of the retrieval error is based on the signal-to-noise ratio (SNR) of the OCO instrument, which is 360, 250, and 180 for a nominal signal (SZA of 60° and surface albedo of 5%) of 15, 2.5 and 1 $W/m^2/sr/\mu m$ for the O_2 A band, the 1.61 μm CO_2 band, and the 2.06 μm CO_2 band, respectively. To degrade the resolving power we increased the assumed width of the entrance slit of the instrument improving the SNR. Both, the calculated retrieval errors and DOFs for CO_2 show a clear dependence on spectral resolution (Figure 8). For this example, a degradation of the resolution by a factor of 16 results in more than a doubling of the retrieval error from 0.55 ppm to 1.3 ppm. At the same time, the DOF drop from 1.55 to less than 1. Nevertheless, in theory the total CO_2 column can still be retrieved with an error in the range of 0.3% for a resolving power of 1250. When X_{CO_2} is retrieved from measured spectra, however, this theoretical limit usually cannot be achieved. Inadequacies in the forward model in describing the measured scene and the instrument condition will add additional scatter to this theoretical limit. Furthermore, for CO_2 and O_2, which have plenty of strong absorption lines, the error budget is dominated by systematic errors and not random errors. The OCO instrument was therefore designed to achieve a resolving power between 17,000 and 20,000 at the price of lower SNR. This high spectral resolving power allows to distinguish individual rotational lines in the measured spectra, so that inadequacies in the forward model can more easily be identified and corrected.

[56] To study the effect of the footprint area on the number of cloud-free soundings, we have aggregated MODIS(Aqua) pixels with an area of 1 km^2 to larger and larger footprint areas centered on Park Falls. The cloud fraction of these footprints can then be determined from the MODIS cloud mask. If 99% of the aggregated MODIS pixels are "confident clear," the sounding has been declared cloud free. Figure 9 illustrates the clear-sky frequency as a function of ground pixel area for April to September 2005. The clear-sky frequency clearly correlates with the area of the ground pixel and drops from 36% for a 3 km^2 pixel area (OCO) to ~15% for a pixel area of 1800 km^2 (SCIAMACHY). For certain months, e.g., April and May, the very strict cloud filter used here reduces the number of available spectra to less than 5%. A reliable cloud filter, as strict as discussed above, is usually not available and most retrievals of observations with large ground pixel area will be compromised to some degree by clouds. Furthermore, variations of aerosol loading and surface characteristics will lead to inhomogeneities within an individual sounding and introduce additional scatter in the retrieval of X_{CO_2}. To minimize these effects and to maximize the number of useful obser-

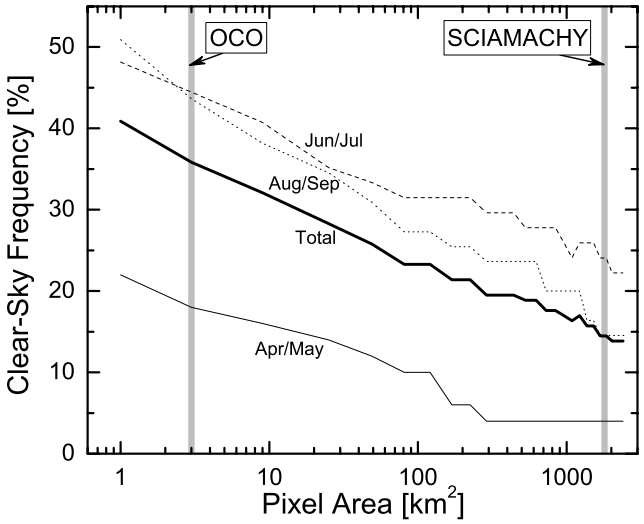

Figure 9. Clear-sky frequency for Park Falls as a function of ground pixel area for April/May, June/July and August/September 2005. The clear-sky frequency has been calculated from the MODIS (Aqua) cloud mask by aggregating MODIS pixels with a spatial resolution of 1 km^2. If 99% of the aggregated MODIS pixels are "confident clear," the sounding has been declared cloud free. The gray-shaded areas reflect the ground pixel size of the OCO and the SCIAMACHY instruments, respectively. Sampling frequencies of the instruments were not taken into account.

vations, the OCO instrument has a footprint area of 3 km^2. Such a small footprint area, however, results in a reduced representativeness of the measurement when compared to model calculations. For a well mixed gas, such as CO_2, with high spatial and temporal correlation, this representativeness error tends to be small and is largely outweighed by the advantages discussed above.

7. Summary and Discussion

[57] We have used SCIAMACHY spectra measured over Park Falls, Wisconsin, from June to October 2004 and February to August 2005 to test the Orbiting Carbon Observatory (OCO) retrieval algorithm and validation concept. Specifically, we have retrieved the column-averaged dry air mole fraction of CO_2 (X_{CO_2}) from space-based SCIAMACHY measurements and from coincident ground-based Fourier Transform Spectrometer measurements of the O_2 A band at 0.76 μm and the 1.58 μm CO_2 band using the same algorithm. Even after adopting super-Lorentzian line shapes to account for inadequacies in our representation of the O_2 A band absorption cross sections (i.e., line mixing and collision-induced absorption), we still obtained a positive bias between SCIAMACHY and FTS X_{CO_2} retrievals of $\sim$3.5%. Additionally, the retrieved surface pressure from SCIAMACHY systematically underestimates measurements of a calibrated pressure sensor at the FTS site. These findings lead us to speculate about inadequacies in the forward model of our retrieval algorithm, which we subsequently studied by a linear error analysis. By assuming a 1% intensity offset in the O_2 A band region for the SCIAMACHY X_{CO_2} retrieval, we significantly improved the spectral fit and achieved better consistency in X_{CO_2} between SCIAMACHY and FTS retrievals and in surface pressure between SCIAMACHY and the pressure sensor measurement. The standard deviation obtained from the correlation of SCIAMACHY and FTS X_{CO_2} is around 6.9 ppm, or 1.8%, which suggests that X_{CO_2} can be retrieved from SCIAMACHY measurements over land surfaces and for low aerosol loading with good precision and without significant biases. We compared the seasonal cycle of X_{CO_2} at Park Falls from SCIAMACHY and FTS retrievals with calculations of the MATCH/CASA model and found good qualitative agreement, with MATCH/CASA underestimating the measured seasonal amplitude. SCIAMACHY observations are similar in viewing geometry and spectral range to those of OCO. However, the spectral and spatial resolutions of SCIAMACHY are each 10–20 times poorer than those of OCO and we argue that in theory significant improvements in precision and accuracy could be obtained from a dedicated CO_2 instrument such as OCO. These measurements would then provide critical data for improving our understanding of the carbon cycle, and carbon sources and sinks.

[58] **Acknowledgments.** This work was supported by the Orbiting Carbon Observatory (OCO) project through NASA's Earth System Science Pathfinder (ESSP) program. We thank ESA and DLR for making available SCIAMACHY Level 1 data. We thank the Netherlands Sciamachy Data Center (NL-SCIA-DC), maintained by KNMI and SRON, for providing us data and processing services. We have used NCEP and ECWMF ERA-40 Reanalysis data provided by the NOAA-CIRES Climate Diagnostics Center, Boulder, Colorado, from their Web site at http://www.cdc.noaa.gov and by the European Centre for Medium-Range Weather Forecasts (ECMWF), respectively. We would like to thank Dan Feldman, Hari Nair, Charles Miller, Ross Salawitch, and Rob Spurr for many fruitful discussions. University of Bremen was funded by DLR/BMBF grant 50EE0027 (SADOS). Research at the Jet Propulsion Laboratory, California Institute of Technology, is performed under contract with NASA.

References

Abdou, W. A., C. J. Bruegge, M. C. Helmlinger, J. E. Conel, S. H. Pilorz, W. Ledeboer, B. J. Gaitley, and K. J. Thome (2002), Vicarious calibration experiment in support of the Multi-angle Imaging Spectroradiometer, *IEEE Trans. Geosci. Remote Sens.*, *40*(7), 1500–1511.

Acarreta, J. R., and P. Stammes (2005), Calibration comparison between SCIAMACHY and MERIS onboard Envisat, *IEEE Geosci. Remote Sens. Lett.*, *2*, 31–35.

Berger, B. W., K. J. Davis, C. X. Yi, P. S. Bakwin, and C. L. Zhao (2001), Long-term carbon dioxide fluxes from a very tall tower in a northern forest: Flux measurement methodology, *J. Atmos. Oceanic Technol.*, *18*, 529–542.

Bousquet, P., P. Peylin, P. Ciais, C. L. Quere, P. Friedlingstein, and P. Tans (2000), Regional changes in carbon dioxide fluxes of land and oceans since 1980, *Science*, *290*(5495), 1342–1346.

Bovensmann, H., J. P. Burrows, M. Buchwitz, J. Frerick, S. Noel, V. V. Rozanov, K. V. Chance, and A. P. H. Goede (1999), SCIAMACHY: Mission objectives and measurement modes, *J. Atmos. Sci.*, *56*, 127–150.

Bowman, K. W., T. Steck, H. M. Worden, J. Worden, S. Clough, and C. Rodgers (2002), Capturing time and vertical variability of tropospheric ozone: A study using TES nadir retrievals, *J. Geophys. Res.*, *107*(D23), 4723, doi:10.1029/2002JD002150.

Buchwitz, M., and J. P. Burrows (2004), Retrieval of CH_4, CO and CO_2 total column amounts from SCIAMACHY near-infrared nadir spectra: Retrieval algorithm and first results, in *Remote Sensing of Clouds and the Atmosphere VIII*, *Proc. SPIE*, vol. 5235, edited by K. Schaefer et al., pp. 375–388, Int. Soc. for Opt. Eng., Bellingham, Wash.

Buchwitz, M., V. V. Rozanov, and J. P. Burrows (2000), A near-infrared optimized DOAS method for the fast global retrieval of atmospheric CH_4, CO, CO_2, H_2O, and N_2O total column amounts from SCIAMACHY Envisat-1 nadir radiances, *J. Geophys. Res.*, *105*, 15,231–15,245.

Buchwitz, M., S. Noel, K. Bramstedt, V. V. Rozanov, M. Eisinger, H. Bovensmann, S. Tsvetkova, and J. P. Burrows (2004), Retrieval of trace gas vertical columns from SCIAMACHY/Envisat near-infrared nadir spectra: First preliminary results, *Adv. Space Res.*, *34*, 809–814.

Buchwitz, M., et al. (2005a), Atmospheric methane and carbon dioxide from SCIAMACHY satellite data: Initial comparison with chemistry and transport models, *Atmos. Chem. Phys.*, *5*, 941–962.

Buchwitz, M., R. de Beek, S. Noel, J. P. Burrows, H. Bovensmann, H. Bremer, P. Bergamaschi, S. Körner, and M. Heimann (2005b), Carbon monoxide, methane and carbon dioxide columns retrieved from SCIAMACHY by WFM-DOAS: Year 2003 initial data set, *Atmos. Chem. Phys.*, *5*, 3313–3329.

Buchwitz, M., et al. (2006), Atmospheric carbon gases retrieved from SCIAMACHY by WFM-DOAS: Version 0.5 CO and CH_4 and impact of calibration improvements on CO_2 retrieval, *Atmos. Chem. Phys.*, *6*, 2727–2751.

Burrows, J. P., E. Holzle, A. P. H. Goede, H. Visser, and W. Fricke (1995), SCIAMACHY—Scanning imaging absorption spectrometer for atmospheric chartography, *Acta Astron.*, *35*, 445–451.

Chahine, M., C. Barnet, E. T. Olsen, L. Chen, and E. Maddy (2005), On the determination of atmospheric minor gases by the method of vanishing partial derivatives with application to CO_2, *Geophys. Res. Lett.*, *32*, L22803, doi:10.1029/2005GL024165.

Chance, K., T. P. Kurosu, and C. E. Sioris (2005), Undersampling correction for array detector-based satellite spectrometers, *Appl. Opt.*, *44*, 1296–1304.

Chédin, A., R. Saunders, A. Hollingsworth, N. Scott, M. Matricardi, J. Etcheto, C. Clerbaux, R. Armante, and C. Crevoisier (2003a), The feasibility of monitoring CO_2 from high-resolution infrared sounders, *J. Geophys. Res.*, *108*(D2), 4064, doi:10.1029/2001JD001443.

Chédin, A., S. Serrar, N. A. Scott, C. Crevoisier, and R. Armante (2003b), First global measurement of midtropospheric CO_2 from NOAA polar satellites: Tropical zone, *J. Geophys. Res.*, *108*(D18), 4581, doi:10.1029/2003JD003439.

Christi, M. J., and G. L. Stephens (2004), Retrieving profiles of atmospheric CO2 in clear sky and in the presence of thin cloud using spectroscopy from the near and thermal infrared: A preliminary case study, *J. Geophys. Res.*, *109*, D04316, doi:10.1029/2003JD004058.

Crevoisier, C., S. Heilliette, A. Chédin, S. Serrar, R. Armante, and N. A. Scott (2004), Midtropospheric CO_2 concentration retrieval from AIRS observations in the tropics, *Geophys. Res. Lett.*, *31*, L17106, doi:10.1029/2004GL020141.

Crisp, D., et al. (2004), The orbiting carbon observatory (OCO) mission, *Adv. Space Res.*, *34*, 700–709.

de Haan, J., P. Bosma, and J. Hovenier (1987), The adding method for multiple scattering calculations of polarized light, *Astron. Astrophys.*, *183*, 371–391.

Denning, A. S., M. Nicholls, L. Prihodko, I. Baker, P.-L. Vidale, K. Davis, and P. Bakwin (2003), Simulated and observed variations in atmospheric CO_2 over a Wisconsin forest, *Global Change Biol.*, *9*, 1241–1250.

Dils, B., et al. (2006), Comparisons between SCIAMACHY and ground-based FTIR data for total columns of CO, CH_4, CO_2 and N_2O, *Atmos. Chem. Phys.*, *6*, 1953–1976.

Dufour, E., F. Bréon, and P. Peylin (2004), CO_2 column averaged mixing ratio from inversion of ground-based solar spectra, *J. Geophys. Res.*, *109*, D09304, doi:10.1029/2003JD004469.

Engelen, R. J., and A. P. McNally (2005), Estimating atmospheric CO_2 from advanced infrared satellite radiances within an operational four-dimensional variational (4D-Var) data assimilation system: Results and validation, *J. Geophys. Res.*, *110*, D18305, doi:10.1029/2005JD005982.

Fan, S., M. Gloor, J. Mahlman, S. Pacala, J. Sarmiento, T. Takahashi, and P. Tans (1998), A large terrestrial carbon sink in North America implied by atmospheric and oceanic carbon dioxide data and models, *Science*, *282*(5388), 442–446.

Frankenberg, C., U. Platt, and T. Wagner (2005), Iterative maximum a posteriori (IMAP)-DOAS for retrieval of strongly absorbing trace gases: Model studies for CH_4 and CO_2 retrieval from near infrared spectra of SCIAMACHY onboard Envisat, *Atmos. Chem. Phys.*, *5*, 9–22.

Geller, M. (1992), A high resolution atlas of the infrared spectrum of the sun and the Earth atmosphere from space, volume III. key to identification of solar features from 650 to 4800 cm^{-1}, *NASA Ref. Publ.*, *1224*.

Geller, M. (1995), Line identification in ATMOS solar spectra, in *Laboratory and Astronomical High Resolution Spectra*, *ASP Conf. Ser.*, vol. 81, edited by A. J. Sauval, R. Blomme, and N. Grevesse, p. 88, Astron. Soc. of the Pac., San Francisco, Calif.

Gerbig, C., J. C. Lin, S. C. Wofsy, B. C. Daube, A. E. Andrews, B. B. Stephens, P. S. Bakwin, and C. A. Grainger (2003), Toward constraining regional-scale fluxes of CO_2 with atmospheric observations over a continent: 1. Observed spatial variability from airborne platforms, *J. Geophys. Res.*, *108*(D24), 4756, doi:10.1029/2002JD003018.

Gurney, K. R., et al. (2002), Towards robust regional estimates of CO_2 sources and sinks using atmospheric transport models, *Nature*, *415*, 626–630.

Hook, S. J. (2000), ASTER spectral library, vol. 1.2. (Available at http://asterweb.jpl.nasa.gov)

Houweling, S., F. Breon, I. Aben, C. Rodenbeck, M. Gloor, M. Heimann, and P. Ciais (2004), Inverse modeling of CO_2 sources and sinks using satellite data: A synthetic inter-comparison of measurement techniques and their performance as a function of space and time, *Atmos. Chem. Phys.*, *4*, 523–538.

Houweling, S., W. Hartmann, I. Aben, H. Schrijver, J. Skidmore, G.-J. Roelofs, and F.-M. Breon (2005), Evidence of systematic errors in SCIAMACHY-observed CO_2 due to aerosols, *Atmos. Chem. Phys.*, *5*, 3003–3013, sref:1680-7324/acp/2005-5-3003.

Intergovernmental Panel on Climate Change (IPCC) (2001), *Climate Change 2001: The Scientific Basis. Contribution of Working Group I to the Third Assessment Report of the Intergovernmental Panel on Climate Change*, edited by J. T. Houghton et al., Cambridge Univ. Press, New York.

Kuang, Z., J. Margolis, G. Toon, D. Crisp, and Y. Yung (2002), Spaceborne measurements of atmospheric CO_2 by high-resolution NIR spectrometry of reflected sunlight: An introductory study, *Geophys. Res. Lett.*, *29*(15), 1716, doi:10.1029/2001GL014298.

Lichtenberg, G., et al. (2005), SCIAMACHY level1 data: Calibration concept and in-flight calibration, *Atmos. Chem. Phys. Discuss.*, *5*, 8925–8977.

Livingston, W., and L. Wallace (1991), An atlas of the solar spectrum in the infrared from 1850 to 9000 cm^{-1} (1.1 to 5.4 micrometer), NSO technical report, Natl. Sol. Obs., National Opt. Astron. Obs., Tucson, Ariz.

Mao, J. P., and S. R. Kawa (2004), Sensitivity studies for space-based measurement of atmospheric total column carbon dioxide by reflected sunlight, *Appl. Opt.*, *43*, 914–927.

Matsueda, H., H. Y. Inoue, and M. Ishii (2002), Aircraft observation of carbon dioxide at 8–13 km altitude over the western Pacific from 1993 to 1999, *Tellus, Ser. B*, *54*, 1–21.

Natraj, V., R. Spurr, H. Bösch, Y. Jiang, and Y. L. Yung (2006), Evaluation of errors from neglecting polarization in the analysis of O_2 A band measurements from space, *J. Quant. Spectrosc. Radiat. Transfer*, doi:10.1016/j.jqsrt.2006.02.073, in press.

Nicholls, M. E., A. S. Denning, L. Prihodko, P. Vidale, I. Baker, K. Davis, and P. Bakwin (2004), A multiple-scale simulation of variations in atmospheric carbon dioxide using a coupled biosphere-atmospheric model, *J. Geophys. Res.*, *109*, D18117, doi:10.1029/2003JD004482.

O'Brien, D. M., and P. J. Rayner (2002), Global observations of the carbon budget: 2. CO_2 column from differential absorption of reflected sunlight in the 1.61 μm band of CO_2, *J. Geophys. Res.*, *107*(D18), 4354, doi:10.1029/2001JD000617.

Olsen, S. C., and J. T. Randerson (2004), Differences between surface and column atmospheric CO_2 and implications for carbon cycle research, *J. Geophys. Res.*, *109*, D02301, doi:10.1029/2003JD003968.

Park, J. H. (1997), Atmospheric CO_2 monitoring from space, *Appl. Opt.*, *36*, 2701–2712.

Pfeilsticker, K., H. Bösch, C. Camy-Peyret, R. Fitzenberger, H. Harder, and H. Osterkamp (2001), First atmospheric profile measurements of UV/visible O_4 absorption band intensities: Implications for the spectroscopy, and the formation enthalpy of the O_2-O_2 dimer, *Geophys. Res. Lett.*, *28*, 4595–4598.

Rayner, P. J., and D. M. O'Brien (2001), The utility of remotely sensed CO_2 concentration data in surface source inversions, *Geophys. Res. Lett.*, *28*, 2429.

Rodgers, C. D. (2000), *Inverse Methods for Atmospheric Sounding: Theory and Practice*, World Sci., Hackensack, N. J.

Rodgers, C. D., and B. J. Connor (2003), Intercomparison of remote sounding instruments, *J. Geophys. Res.*, *108*(D3), 4116, doi:10.1029/2002JD002299.

Rothman, L. S., et al. (2005), The HITRAN 2004 molecular spectroscopic database, *J. Quant. Spectrosc. Radiat. Transfer*, *96*, 139–204.

Shettle, E. P., and R. W. Fenn (1979), Models for the aerosols of the lower atmosphere and the effects of humidity variations on their optical properties, *AFGL Tech. Rep.*, *AFGL-TR-79-0214*.

Strow, L. L., S. E. Hannon, M. Weiler, K. Overoye, S. L. Gaiser, and H. H. Aumann (2003), Prelaunch spectral calibration of the Atmospheric Infrared Sounder (AIRS), *IEEE Trans. Geosci. Remote Sens.*, *41*(2).

Tans, P. P. (1996), Carbon cycle (group report), in *Summary Report 1994–1995*, vol. 23, Clim. Monit. and Diagnost. Lab., U.S. Dep. of Commer., Boulder, Colo.

Tans, P. P., and T. J. Conway (2005), Monthly atmospheric CO_2 mixing ratios from the NOAA CMDL carbon cycle cooperative global air sampling network, 1968–2002, in *A Compendium of Data on Global Change*, Carbon Dioxide Inf. Anal. Center, Oak Ridge Natl. Lab., U.S. Dep. of Energy, Oak Ridge, Tenn.

Toon, G. C., J.-F. Blavier, B. Sen, R. J. Salawitch, G. B. Osterman, J. Notholt, M. Rex, C. T. McElroy, and J. M. Russell III (1999), Ground-based observations of Arctic ozone loss during spring and summer 1997, *J. Geophys. Res.*, *104*, 26,497–26,510.

Tran, H., C. Boulet, and J.-M. Hartmann (2006), Line mixing and collision-induced absorption by oxygen in the A band: Laboratory measurements, model, and tools for atmospheric spectra computations, *J. Geophys. Res.*, *111*, D15210, doi:10.1029/2005JD006869.

Vallance Jones, A., and R. Gattinger (1963), The seasonal variation and excitation mechanism of the 1.58 $\mu^1\Delta_g - {}^3\Sigma_g^-$ twilight airglow band, *Planet. Space Sci.*, *11*, 961.

van Diedenhoven, B., O. P. Hasekamp, and I. Aben (2005), Surface pressure retrieval from SCIAMACHY measurements in the O_2 A band: Validation of the measurements and sensitivity on aerosols, *Atmos. Phys. Chem.*, *5*, 2109–2120.

Wallace, L., K. Hinkle, and W. C. Livingston (1993), An atlas of the photospheric spectrum from 8900 to 13600 cm^{-1} (7350 to 11230), NSO technical report, Natl. Sol. Obs., Tucson, Ariz.

Warneke, T., R. de Beek, M. Buchwitz, J. Notholt, A. Schulz, V. Velazco, and O. Schrems (2005a), Shipborne solar absorption measurements of CO_2, CH_4, N_2O and CO and comparison with SCIAMACHY WFM-DOAS retrievals, *Atmos. Chem. Phys.*, *5*, 2029–2034.

Warneke, T., Z. Yang, S. Olsen, S. Krner, J. Notholt, G. C. Toon, V. Velazco, A. Schulz, and O. Schrems (2005b), Seasonal and latitudinal variations of column averaged volume-mixing ratios of atmospheric CO_2, *Geophys. Res. Lett.*, *32*, L03808, doi:10.1029/2004GL021597.

Washenfelder, R. A., P. O. Wennberg, and G. C. Toon (2003), Tropospheric methane retrieved from ground-based near-IR solar absorption spectra, *Geophys. Res. Lett.*, *30*(23), 2226, doi:10.1029/2003GL017969.

Washenfelder, R. A., G. Toon, J.-F. Blavier, Z. Yang, N. Allen, P. Wennberg, S. Vay, D. Matross, and B. Daube (2006), Carbon dioxide column abundances at the Wisconsin tall tower site, *J. Geophys. Res.*, *111*, D22305, doi:10.1029/2006JD007154.

Wiscombe, W. J. (1980), Improved Mie scattering algorithms, *Appl. Opt.*, *19*, 1505–1509.

Yang, Z., G. C. Toon, J. S. Margolis, and P. O. Wennberg (2002), Atmospheric CO_2 retrieved from ground-based near IR solar spectra, *Geophys. Res. Lett.*, *29*(9), 1339, doi:10.1029/2001GL014537.

Yang, Z., P. O. Wennberg, R. P. Cageao, T. J. Pongetti, G. C. Toon, and S. P. Sander (2005), Ground-based photon path measurements from solar absorption spectra of the O_2 A-band, *J. Quant. Spectrosc. Radiat. Transfer*, *90*, 309–321.

H. Bösch, D. Crisp, B. Sen, and G. C. Toon, Jet Propulsion Laboratory, California Institute of Technology, MS 183-601, 4800 Oak Grove Drive, Pasadena, CA 91109-8099, USA. (hartmut.boesch@jpl.nasa.gov)

M. Buchwitz, J. P. Burrows, and R. de Beek, Institute of Environmental Physics, University of Bremen, Otto-Hahn-Allee 1, D-28359 Bremen, Germany.

M. Christi, Department of Atmospheric Science, Colorado State University, Fort Collins, CO 80523, USA.

B. J. Connor, National Institute of Water and Atmospheric Research, PB 50061, Omakau, Lauder, Otago, 9182, New Zealand.

V. Natraj, R. A. Washenfelder, P. O. Wennberg, and Y. L. Yung, Division of Geological and Planetary Sciences, California Institute of Technology, 1200 East California Blvd., Pasadena, CA 91125, USA.